Polypropylene-based Composites Reinforced with Waste Tropic Wood Flours: Determination of Accelerated Weathering Resistance, Tribological, and Thermal Properties

İbrahim Halil Başboğa *

This study investigated the effects of Iroko wood flour (WF) and nano-titanium dioxide (TiO_2) concentration on the properties of polypropylene (PP)-based composites, including accelerated weathering resistance, tribological behavior, thermal stability, physical characteristics, mechanical strength, morphological features, color changes, and surface roughness. The results showed that the presence of WF and TiO_2 significantly influenced the density, hardness, thermal stability, crystallinity, coefficient of friction, and wear rate of the composites. Both fillers positively impacted the tensile strength, flexural strength, and flexural modulus of the composites, although the elongation at break values decreased. TiO_2 addition enhanced thermal stability and protection against UV radiation, whereas using wood flour negatively affected color properties. Moreover, the surface roughness of the composites was affected by weathering time and wood flour content. These findings highlight the potential of WF and TiO_2 as effective fillers for enhancing PP-based composites' properties and weathering resistance.

DOI: 10.15376/biores.18.4.7251-7294

Keywords: Wood-plastic composite; Iroko wood flour; UV aging; Tribological properties

*Contact information: Department of Forest Industry Engineering, Faculty of Forestry, Bursa Technical University, 16310, Bursa, Türkiye; *Corresponding author: ibrahim.basboga@btu.edu.tr*

INTRODUCTION

Wood-plastic composites (WPCs) refer to materials obtained by incorporating wood or other lignocellulosic materials into thermoplastic matrices in varying sizes and proportions (Klyosov 2007; Behravesh *et al.* 2010). Over the past decade, there has been a growing interest in producing composite materials. Carus and Eder (2015) anticipate a substantial growth trajectory, projecting a remarkable increase from a modest 10,000 tonnes in 2012 to a significant 100,000 tonnes by 2020, owing to enhanced technical attributes, reduced costs, and strengthened supplier networks facilitating robust customer support. Furthermore, the global WPC market projection is predicted to reach 9,953.8 million US dollars by 2028, with a value of approximately 4,033.5 million US dollars in 2018 and exhibit a healthy growth rate of over 9.5% during the forecast period of 2021 to 2030 (Johnson 2020). These statistics highlight the remarkable growth and promising future of the WPC market.

Numerous studies have focused on the utilization of wood flours, residues from various wood species, agricultural and industrial waste, and numerous lignocellulosic materials in the production of WPCs (Mengeloglu and Kabakci 2008; Başboğa *et al.* 2020, 2022; Çavuş 2020; Çavuş and Mengeloğlu 2020; Tasdemir *et al.* 2020; Boran Torun *et al.* 2021; Dönmez Çavdar *et al.* 2021; Mrówka *et al.* 2021). These studies have contributed significantly to understanding the potential feedstock materials and their utilization in the production of WPCs. Extensive research has investigated the characteristics of WPCs produced by blending various thermoset or thermoplastic polymers with different lignocellulosic fillers. These studies explored the potential of WPCs as environmentally friendly alternatives to traditional materials in various industries, including construction, automotive, and packaging. The combination of polymers with lignocellulosic fillers offers the advantage of utilizing renewable resources while enhancing the composites' mechanical properties, thermal stability, and overall performance. Understanding the synergistic effects between different polymers and fillers is essential for optimizing WPCs' formulation and manufacturing processes, thus enabling their widespread usage as sustainable materials.

The WPCs are commonly preferred for applications in outdoor environments, such as garden furniture and wetted surfaces. Combining wood fibers or other lignocellulosic materials with thermoplastic matrices offers several advantages that make WPCs well-suited for these specific applications. Their inherent resistance to moisture, decay, weathering, and ability to withstand harsh outdoor conditions make them an ideal choice for outdoor settings. Additionally, WPCs provide an aesthetically pleasing alternative to traditional materials because they can mimic the appearance of natural wood while offering enhanced durability and low maintenance requirements. The utilization of WPCs in these contexts addresses the demand for sustainable materials and provides functional and visually appealing solutions for various outdoor applications.

Many studies have been conducted to determine the weathering properties of WPCs (Du *et al.* 2010; Teacă *et al.* 2013; Peng *et al.* 2014; Chen *et al.* 2016; Badji *et al.* 2017; Aydemir *et al.* 2019; Boran Torun *et al.* 2021; Dönmez Çavdar *et al.* 2021; Mengeloğlu and Çavuş 2021). Determining the aging properties of WPCs holds paramount importance in assessing these materials' long-term performance and durability. Aging processes, such as exposure to environmental factors, ultraviolet (UV) radiation, moisture, temperature variations, and mechanical stress, can significantly influence WPCs' structural integrity and functional properties. Understanding the effects of aging on WPCs is crucial for ensuring their suitability in outdoor applications with challenging weather conditions and prolonged exposure to UV radiation. Studying aging characteristics provides valuable insights into the degradation mechanisms, dimensional stability, color changes, mechanical strength, and overall service life of WPCs. Moreover, this knowledge aids in developing effective strategies for material formulation, manufacturing processes, and protective treatments to enhance WPCs' long-term durability and performance in real-world applications.

Despite extensive research conducted on various attributes of WPCs, the number of studies aimed at determining coefficient of friction (CoF) and wear rate (WR) properties remains limited. The majority of previous studies in this field have focused on composites produced by incorporating lignocellulosic fillers with thermoset polymers (Dwivedi and Chand 2008; Yousif and El-Tayeb 2008/2010; Nirmal *et al.* 2010; Ahalwan and Yousif 2013; Latha *et al.* 2016; Richard *et al.* 2017; Ranakoti *et al.* 2019; Mylsamy *et al.* 2020). Furthermore, in another study, three different liquid solutions were impregnated into wood, and their wear properties were examined (Hamdan *et al.* 2010). Even fewer publications have been dedicated to the study of tribological properties of thermoplastic polymers and their composites incorporating natural fillers, including materials such as polyoxymethylene (Li *et al.* 2008; Xiang *et al.* 2012), polyethylene (Brostow *et al.* 2016; Yang *et al.* 2019; Al-Maqdasi *et al.* 2022), polyvinyl chloride (Jiang *et al.* 2017; Jiang *et al.* 2018), polypropylene (Aurrekoetxea *et al.* 2008; Bajpai *et al.* 2012; Mysiukiewicz and Sterzyński 2017; Ibrahim *et al.* 2019; Mazzanti *et al.* 2021), and polylactic acid (Mysiukiewicz and Sterzyński 2017). Despite the limited number of studies on the subject, a previous investigation indicated that the addition of wood flour reduced the CoF compared to the neat polymer (Aurrekoetxea *et al.* 2008). The potential usage of WPCs as sliding or frictional materials in bearing production is highlighted by the decreased CoF resulting from the inclusion of natural fibers. The two main components of WPCs, polymer and wood, are commonly already employed in bearing production (Mysiukiewicz and Sterzyński 2017).

The high demand for tropical wood species in Turkey includes Iroko (*Chlorophora excelsa*), Dahoma/Dabema, Sapelli, Sipo, Acajou (Akaju/Khaya), Ayous, Limba (White frake), and Afrormosia timber (Ekşioğlu 2022). Iroko wood is highly regarded for its exceptional mechanical and physical properties, making it widely utilized for structural components (Ouinsavi *et al.* 2005; Geert and Kuilen 2010). Following European standards, Iroko wood is classified as strength class D40, as defined in EN 338 (2009). The utilization of Iroko wood in construction and other industries is rising because of its robust nature and ability to withstand heavy loads and environmental factors. The remarkable mechanical and physical properties of Iroko wood make it a desirable choice for structural elements, contributing to the overall strength and durability of the constructed components. Iroko wood finds applications in decorative veneers, furniture production, interior and exterior decorations, solid parquet manufacturing, boat building, manufacturing of industrial kitchen materials, industrial or heavily used flooring, as well as in flooring for docks and piers, staircase construction, and furniture components. Iroko timber exhibits remarkable resistance to natural conditions, such as water, moisture, and sunlight, making it a preferred choice for outdoor furniture used extensively in parquet, boat, yacht, ship, and deck construction (Ekşioğlu 2022). The sawing process of these woods generates a substantial amount of sawdust. Additionally, cutting and furniture manufacturing produces unused small wood particles as waste, leading to wastage.

This research aimed to examine the impact of incorporating Iroko wood flour as filler in the production of wood-plastic composites (WPCs) on their technological properties. Furthermore, the study investigated the effects of incorporating nano TiO_2, which has demonstrated UV radiation resistance in previous studies (Hazarika and Maji 2013), combined with Iroko wood flour as a filler. Additionally, while there have been several types of research on the determination of tribological properties in metal and polymer composites, more studies need to focus on assessing these properties in WPCs. The utilization of natural fibers within WPCs, leading to improved CoF properties (Aurrekoetxea *et al.* 2008) and the potential of TiO_2 as a promising lubricating filler for enhanced engine efficiency (Birleanu *et al.* 2022), have served as sources of inspiration for this study. Hence, this study also aims to evaluate the influence of fillers on the friction coefficient and wear rate of WPCs.

EXPERIMENTAL

Materials

In this study, commercial polypropylene (PP) (product code: EH-102) was used as a thermoplastic matrix and purchased from PETKİM Petrochemical Company in İzmir, Türkiye. The general properties of PP coded with EH-102 are presented in the PETKİM Petrochemical Company data sheet (Petkim 2016).

Wood flours of the Iroko (*Chlorophora excelsa*) tree, which is a tropical species, were used as lignocellulosic filler. The Iroko waste flours were obtained from a company that produces industrial kitchens, which is a company operating in the Kısıkköy furniture region in İzmir, Türkiye. The sawdust and the leftover pieces that emerged while sawing the timber and during the production of furniture were utilized as the filler. Iroko wood wastes with an average air-dry density of 0.575±0.026 g/cm^3 were granulated into different mesh-sized flour by Wiley mill and dried before production. Iroko flours (WF) were screened and passed through a 20-mesh sieve and retained on an 80-mesh sieve were used. The WF dimensions were approximately in the size range of 0.71 to 0.177 mm. Nano-sized titanium dioxide (TiO_2) was purchased from KIMETSAN Ltd. Co. (Ankara, Türkiye). TiO_2 was used to increase the resistance of the WPCs against UV rays. The general properties of TiO_2 are given in Table 1.

Table 1. General Properties of TiO_2

Properties	TiO_2
Appearance	White, Powder
Purity	99.7%
Average Particle Size	25 ± 5 nm
Surface Area	72 m^2/g
Bulk Density	0.22 g/cm^3
Density at 25 °C	3.9 g/cm^3
pH	7
Mass Loss on Drying 105 °C for 2 months	5%
Mass Loss on Ignition	3%

To increase the interface interaction between the hydrophobic polymer matrix and the hydrophilic lignocellulosic filler, maleic anhydride grafted polypropylene (MAPP) (Licomont AR 504 by Clariant, Muttenz, Basel, Switzerland) was used as a coupling agent, and Paraffin-wax (K.130.1000) was used as a lubricant. The general properties of coupling agent and lubricant are presented in Table 2.

Table 2. General Properties of MAPP and Paraffin-wax

Properties	Licomont AR 504 (MAPP)	Properties	Paraffin-wax
Appearance	Yellowish, fine-grained	**Appearance**	White, Powder
Softening Point	156 °C	**Softening Point**	56 to 58 °C
Density (23 °C)	0.91 g/cm^3	**Density (23 °C)**	0.93 g/cm^3
Viscosity (140 °C)	800 mPa.s	**Chemical Formula**	C18H38
Acid value	41 mg KOH/g	**Commercial name**	Paraffin-wax

Polymer Composite Production by Injection Molding

The manufacturing of waste Iroko-filled and PP-based WPCs was completed in two stages. In the first stage, composite pellets were produced by the extrusion method, and then in the second stage, composite test samples were produced from these pellets by the injection molding method. The manufacturing schedule of the study is given in Table 3.

Table 3. The Manufacturing Schedule of WPCs

ID	PP Amount (%)	Iroko Wood Waste Flours (WF) (%)	Titanium Dioxide (TiO_2) (%)
W0T0	97	0	0
W0T3	94	0	3
W0T6	91	0	6
W0T9	88	0	9
W20T0	77	20	0
W20T3	74	20	3
W20T6	71	20	6
W20T9	68	20	9
W40T0	57	40	0
W40T3	54	40	3
W40T6	51	40	6
W40T9	48	40	9

Iroko waste wood flours (WF) were dried in an oven so that the resulting moisture content was close to zero before manufacturing. Depending on the formulation given, PP, WF, TiO_2, MAPE, and paraffin wax were dry-mixed in a high-intensity mixer to produce a homogeneous blend. In all groups, MAPP was used as 3% of the total weight, while paraffin wax was used as an extra 3% of the total weight. Subsequently, the blends were compounded under heat. Compounding was completed with the help of a laboratory-type extruder with a single screw and five different temperature zones. The screw speed was 60 rpm, and extruder temperatures were 195, 190, 185, 180, and 180 °C from the feed zone to the die zone. A water pool was used to cool the extruded compounds. The cooled mixtures were granulated into pellets in the pellet machine. The pellets were kept in a drying oven at 103 °C (± 2) to reach an oven-dry weight before manufacturing WPC samples by injection molding. The standard test samples were produced with HDX-88 Injection Molding Machine. The dried pellets were converted into WPC test specimens under heat and pressure by injection molding method. The temperatures were 180, 190, and 200 °C from the feed zone to the die zone, and the pressure was 102 kg/cm^2. The injection speed and screw speed were 80 mm/s and 40 rpm, respectively. The WPC specimens were injected with a cooling time of about 30 s. Before testing, test specimens were conditioned at 23 ± 2 °C and 50 ± 5% relative humidity for 72 h in a climate chamber. At least 5 samples were tested for the determination of each property of WPCs.

Determination of Physical Properties

Density was measured according to ASTM D792 (2008) water displacement technique using test specimens in the size of 20 mm × 20 mm × 4 mm. The hardness properties of samples were determined accordance with ASTM D2240 (2017) by ENPQIX EHS5D Durometer (Shore D) (Polygon Co., Shenzhen, China).

Determination of Thermal and Morphological Properties

To determine the thermal properties of the PP-based composites, thermogravimetric analysis (TGA) and differential scanning calorimetry (DSC) analysis were conducted with Shimadzu TGA-50 thermal analyzer and Shimadzu DSC-60, respectively. The TGA of the samples was performed at a heating rate of 10 °C/min under nitrogen with 100 mL/min flow rate. The samples were heated from room temperature to 600 °C. The temperature increased from 10 to 200 °C at a heating rate of 10 °C/min during the DSC analysis. The analysis was performed as both cooling and heating according to the isotherm points. The DSC analysis was performed on approximately 10 mg of the sample under a dry nitrogen atmosphere with a 100 mL/min flow rate. The degree of crystallinity (Xc %) was specified from the second melting enthalpy values using the following Eq. 1,

$$X_c(\%) = \frac{\Delta H_m}{(1-\alpha) * \Delta H_c} * 100 \quad (1)$$

where X_c (%) is the crystallinity value, ΔH_m (J/g) is the melting enthalpy of the specimens, ΔH_c (207 J/g) is the enthalpy value of melting of a 100% crystalline form of polypropylene (PP) (Erem *et al.* 2013; Alsan 2016; Bazan *et al.* 2021; Rivera-Armenta *et al.* 2022), and (1-α) is the weight fraction of polymer into the composite material.

The morphology of the composites was characterized using a scanning electron microscope (SEM) (Nova NaNoSEM 650, FEITM, Hillsboro, OR, USA) with the help of the Everhart–Thornley detector (ETD). Before the analysis, the composite samples were dipped into liquid nitrogen and then broken in half to prepare the fractured surfaces. The gold powders were sputtered to the fractured surfaces by Desk V Coater (Desk V, Denton Vacuum Co., Moorestown, NJ, USA) at 10 mA for 120 s to provide electrical conductivity. In addition, a compositional back-scattered detector (CBS), which is one of the back-scattered electron (BSE) detectors, was used for contrast depending on the atomic number to determine the presence of TiO_2 in the WPCs. The SEM analyses were also conducted on unweathered and weathered samples to show the effects of accelerated weathering.

Determination of Tribological Properties

Wear tests were performed with the help of a pin-on-disc machine. An AISI 1040 steel disc with 10-mm thickness and 60-mm diameter, and a hardness value of 50 to 55 HRC was used as a counter-disc material against WPCs. The ASTM G99-17 (2017) standard generally recommends a ground surface roughness of 0.8 µm (R_a) or less. Surface roughness values of steel discs were determined between 0.259 to 0.443 (R_a, µm). Wear tests were conducted at room temperatures (23 °C ± 2 and 48 ± 2% humidity) under dry conditions adapted from the ASTM G99-17 (2017) standard. Tribological tests were performed at two different loads (30 and 60 N) and 1.0 m/s sliding speeds. Wear (K_o) was calculated using the following Eq. 2,

$$K_o = \frac{\Delta m}{L \times F \times p} \quad (2)$$

where Δm is the average weight loss (g), L is the distance (m), F is the load (N), and ρ is the density (g/cm^3).

Determination of Mechanical Properties

The mechanical strength (flexural (ASTM D790 2010), tensile (ASTM D638 2010), and impact (ASTM D256 2010) properties) of the WPC samples was determined according to the relevant standards. The performing of mechanical tests of composites was detailed by Başboğa *et al.* (2020). The variation ratios of flexural and tensile strengths (Eq. 3), the variation ratios of flexural modulus (Eq. 4), and the variation ratios of impact strength (Eq. 5) were calculated:

$$MOR_{Var\ ratio} = \frac{MOR_{after} - MOR_{before}}{MOR_{before}}\ X\ 100 \tag{3}$$

$$MOE_{Var\ ratio} = \frac{MOE_{after} - MOE_{before}}{MOE_{before}}\ X\ 100 \tag{4}$$

$$IS_{Var\ ratio} = \frac{IS_{after} - IS_{before}}{IS_{before}}\ X\ 100 \tag{5}$$

In the above equations, ‘before’ refers to the average strength and modulus values measured before weathering, and ‘after’ refers to the average strength and modulus values measured after weathering. IS refers to impact strength.

Accelerated Weathering Properties

All composite groups were exposed to accelerated weathering conditions in the accelerated weathering test chamber (Atlas UV Test, Mount Prospect, IL, USA). To simulate outdoor aging, accelerated outdoor testing was performed according to procedure 1 based on the ASTM G154 (2011) standard. The WPCs were exposed to UV light for 672 h with variable cycles of temperatures and humidity. The test was performed using 340 nm fluorescent at 0.89 W/m^2/nm irradiance, 8 h of UV light at 60 (± 3) °C, followed by a 4-h condensation treatment cycle at 50 (± 3) °C. Because the first hours are important for the changes in the sample's surface exposed to the accelerated weathering test, measurements were realized on the samples every 24 h for 168 h. Afterwards, surface properties were determined every 168 h and a total of 8 measurements were made from the beginning. Color and surface roughness measurements were recorded as surface properties.

The color coordinates (L^*, a^*, and b^*) were determined over an 8 mm diameter spot from five different points (every time from the same points) with 10° observer angle. Color measurements were realized with the help of a Minolta CM-2600 D spectrophotometer (Konica Minolta, Tokyo, Japan), with 5 different samples (unweathered and weathered) for each group and a total of 25 different measurements. Total color change (ΔE^*) was calculated with the help of Eq. 6 below according to ASTM D2244-22 (2009):

$$\Delta E^* = \sqrt{(\Delta L^*)^2 + (\Delta a^*)^2 + (\Delta b^*)^2} \tag{6}$$

where $\Delta L^*$is the change in lightness and darkness values after weathering (L_2^*- L_1^*), Δa^* is the change in red and green color values after weathering (a_2^* - a_1^*), and $\Delta b^*$is the change in yellow and blue color values after weathering (b_2^* - b_1^*).

The surface roughness of the control and weathered groups samples were determined with a stylus-type diamond tip profilometer (Mitutoyo Surftest SJ-310, Sakado, Japan) according to guidelines provided by ISO 21920-2 (2021) standard, which was revised ISO 4287:1997 (ISO-21920-2 2021). To detect the roughness on the surface, measurements were carried out periodically at the same intervals (24, 48, 72, 96, 120, 144, 168, 336, 504, and 672 h) on the surfaces of the samples exposed to UV degradation.

Measurements were realized from 3 different points for arithmetic average roughness (Ra) values on surfaces of 5 different samples from neat PP and wood and nano-TiO_2 filled wood-plastic composite groups. A total of 15 measurements were taken for each group. A cutoff length (λ_c) of 8 mm, a cutoff wavelength of 8 µm, and a tracing length of 16 mm, was employed for the roughness test.

Statistical Analysis

Design-Expert® Version 7.0.3 (State-Ease, Inc., Minneapolis, MN, USA) and Minitab 19 (Pennsylvania State University, State College, PA, USA) statistical software packages were utilized to specify the interaction of waste Iroko wood flour and TiO_2 amounts on the technological properties of PP-based composites and to discover the extent of statistical significance of impact of filler amounts on surface roughness parameter following the weathering cycles. Two-way analysis of variance (ANOVA) tests were performed to observe the effects of the filler amounts on the technological properties of the samples and effect of weathering and filler amounts on physical properties. For the surface roughness analyses, stepwise regression method was preferred at the 95% confidence level.

RESULTS AND DISCUSSION

In this study, mechanical (tensile, flexural, and impact strength), physical (density and hardness), thermal (TGA, DSC), morphological (SEM), tribological, color change, and surface roughness properties of all PP-based composite groups filled with waste Iroko wood flours (WF) and TiO_2 were determined. All properties were examined under separate headings, and the findings were statistically analyzed and presented graphically under these headings.

Density of WPCs

The average density values of WPCs are given in Table 4.

Table 4. Average Density Values of WPCs

ID	Density (g/cm^3)
W0T0	0.893 (0.004)*
W0T3	0.904 (0.008)
W0T6	0.923 (0.005)
W0T9	0.950 (0.003)
W20T0	0.918 (0.007)
W20T3	0.948 (0.004)
W20T6	0.975 (0.005)
W20T9	0.995 (0.005)
W40T0	0.978 (0.008)
W40T3	1.029 (0.006)
W40T6	1.046 (0.011)
W40T9	1.076 (0.016)

*The numerical value in the parenthesis is standard deviation

A density interaction graph showing the effects of fillers on the density properties of WPCs is also presented in Fig. 1. When the density interaction graph in Fig. 1 was examined, it was determined that both fillers had a significant effect on the density values ($P < 0.0001$). As shown in the interaction graph, the density values show an increase with the addition of WF and TiO_2. Even the usage of TiO_2 at low amounts had a significant effect on the density values. The density value of PP, which is a polymer matrix, is given as 0.905 g/cm^3 in the factory data sheet. In addition, the average density values of the control group samples (without filler) were determined as 0.893 g/cm^3. Moreover, the density value of TiO_2 is given as 3,900 g/cm^3 in the factory data sheet. TiO_2 has a high-density value, even at low levels of usage in the polymer matrix with a much lower density; it was effective on the density values because the density of TiO_2 was much higher than the polymer matrix. From this point of view, the presence of nanomaterial in the WPCs has been demonstrated, and it has been possible to say that a large part of the nanomaterial is contained in the matrix while mixing in the high-speed mixer.

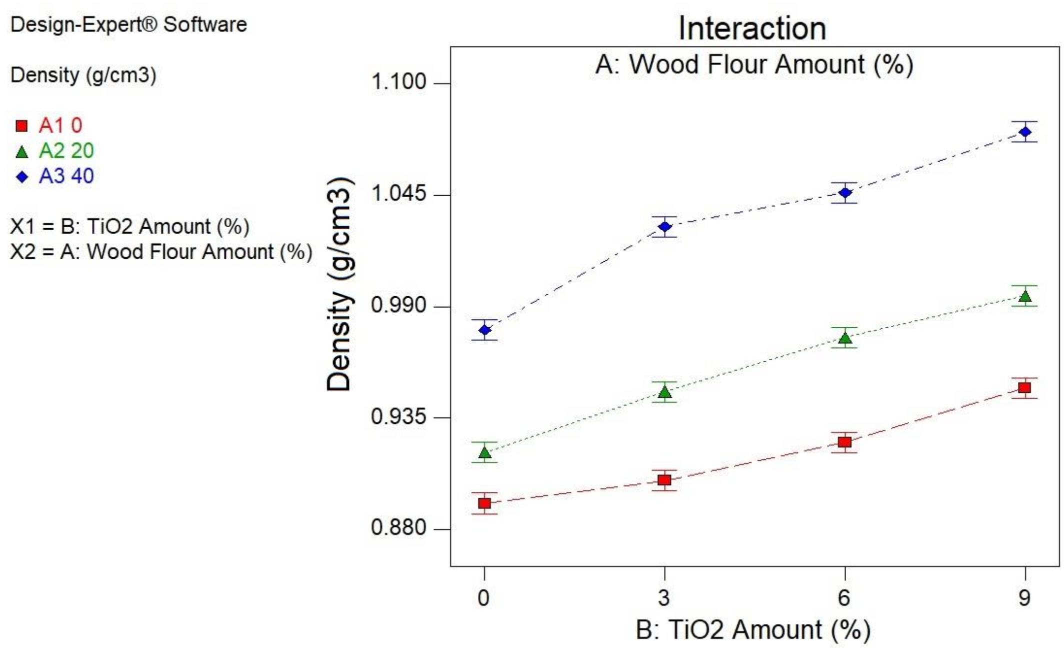

Fig. 1. WF and TiO_2 loadings effects on density of PP-based composites

Furthermore, SEM images were taken at 5000× with the help of a compositional back-scattered detector (CBS) to determine the presence of TiO_2 in the WPCs. The SEM images of all TiO_2 usage amounts of WPC groups with the highest percentage of wood flour (40%) are presented in Fig. 2.

When the SEM images of the W40T0 group (without nanomaterial) in Fig. 2-a are examined, it can be seen that there are no reflecting or back-flare images. Only wood flour pieces that had pulled out of the matrix are visible. However, when the images in Fig. 2-b/c/d are examined, it can be seen that the intensity of the flare in the images rose with the increase in the usage amount of the nanomaterial. These images supported the presence of TiO_2 in WPCs. However, some small agglomerations were determined in some areas of fractured surfaces of WPCs containing nanomaterials at high levels, such as 6% and 9%. These images support the increment of density values of WPCs with TiO_2 loading.

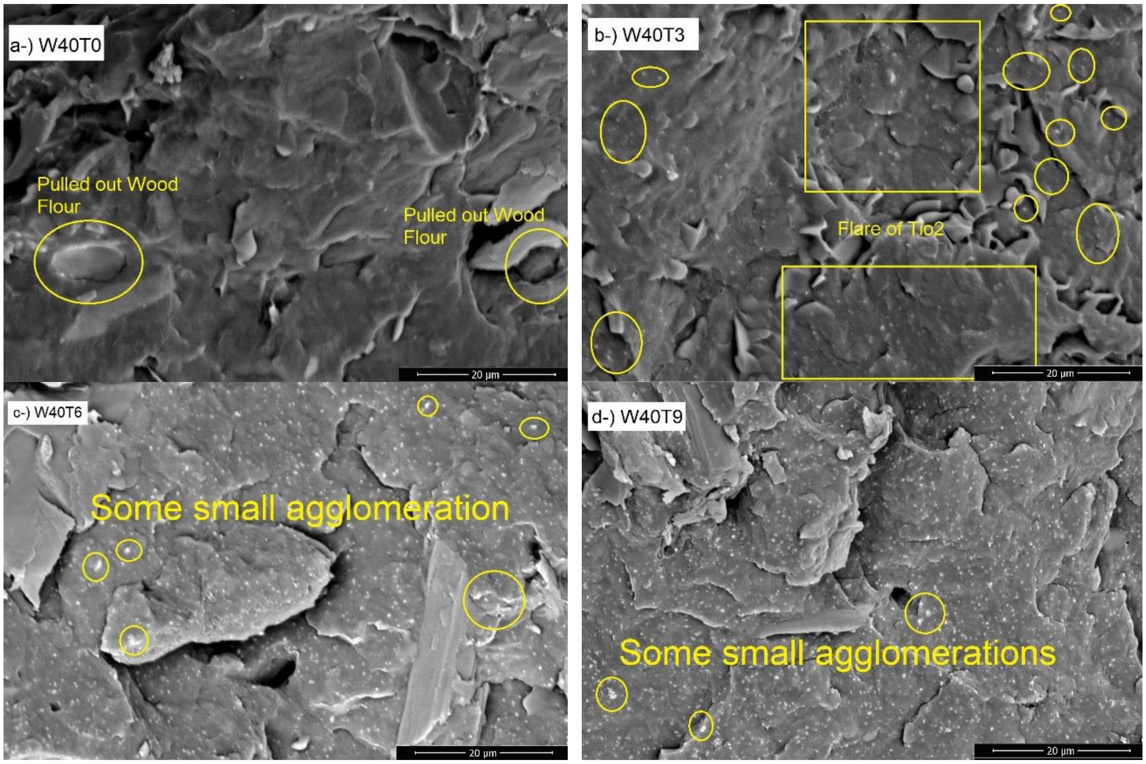

Fig. 2. SEM Images (taken at 5000 magnification) of WPCs containing 40% Iroko Flour and different amounts of TiO_2 taken with a CBS detector: a-) W40T0, b-) W40T3, c-) W40T6, and d-) W40T9

The density values of the WPCs prominently increased with the addition of wood flours. It is believed that a higher density of lignocellulosic Iroko wood flour, which has a high cell wall density, might be responsible for the increased density of the WPCs (Mengeloglu and Karakus 2008; Mengeloğlu *et al.* 2015).It is reported that the usage of lignocellulosic materials as a filler increases the density of PP-based (Steckel *et al.* 2007; Özdemir *et al.* 2013; Mengeloğlu *et al.* 2015; Mazzanti *et al.* 2016; Basalp *et al.* 2020; Mengeloğlu and Çavuş 2021) and HDPE-based (Ramezani Kakroodi *et al.* 2013; Başboğa *et al.* 2020) composites. PP-based WF and TiO_2-filled composites were produced in the density range of 0.893 to 1.076 g/cm^3. The highest average density value was obtained in the composite group, in which fillers were used at the highest level, while the lowest value was obtained in the neat PP group. Higher increases in density values were observed when wood flour and TiO_2 were used at the highest amounts. Moreover, this is generally explained by the rule of mixtures in the literature (Matuana *et al.* 1998; Mengeloğlu and Karakuş 2008; Mengeloğlu and Çavuş 2021). Composite materials obtained by combining high-density fillers and low-density polymer matrix have a higher density compared to the polymer itself (Çavuş and Mengeloğlu 2020; Mengeloğlu and Çavuş 2021). There are similar studies in the literature in which the density values of composites increase with the increment in the amount of filler (Klyosov 2007; Mengeloğlu *et al.* 2015; Çavuş and Mengeloğlu 2016; Mengeloğlu and Çavuş 2021).

Hardness Properties of WPCs

The hardness (Shore D) values of WPCs were determined by an ENPQIX EHS5D durometer (Polygon Co., Shenzhen, China), and the average values are summarized in Table 5.

Table 5. Average Hardness Values of WPCs

ID	Hardness (Shore D)
W0T0	61.30 (2.45)
W0T3	65.67 (0.49)
W0T6	68.40 (1.05)
W0T9	68.03 (3.22)
W20T0	69.40 (0.92)
W20T3	70.47 (0.86)
W20T6	71.99 (2.50)
W20T9	71.30 (0.10)
W40T0	70.70 (1.15)
W40T3	71.90 (0.26)
W40T6	73.03 (1.07)
W40T9	73.87 (1.47)

*The numerical value in the parenthesis is standard deviation

An interaction graph showing the effects of fillers on the hardness properties of composites is given in Fig. 3. Considering the interaction graph, it was determined that both fillers were significantly effective on the hardness values of the composite materials ($P < 0.0001$). The hardness values were enhanced with the usage of both fillers. The hardness values continued to rise with increasing amount of fillers used. Similar results were also reported by Çavuş (2017). The highest hardness value was determined as 73.9 in the W40T9 group containing the highest amount of fillers, and the lowest hardness value was 61.3 in the pure polymer (W0T0) group without fillers.

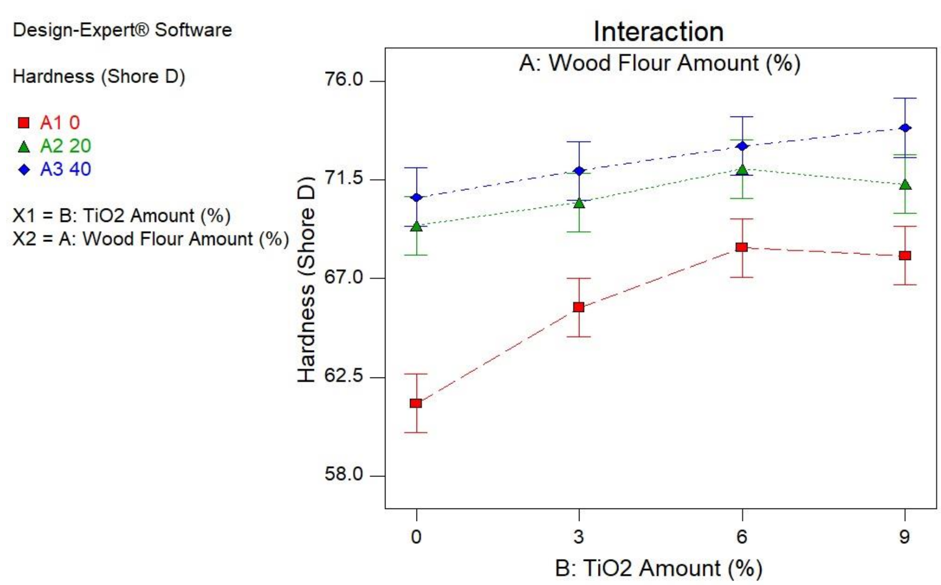

Fig. 3. WF and TiO_2 loadings effects on hardness of PP-based composites

Thermal and Morphological Properties of WPCs

The TGA analyses were performed on six different groups (W0T0, W20T0, W40T0, W40T3, W40T6, and W40T9). The thermal degradation results of WF and TiO_2-reinforced PP-based composites are summarized in Table 6.

Table 6. TGA Results of WF and TiO_2-reinforced PP-based Composites

ID	1st Onset Temp. (°C)	1st Endset Temp. (°C)	2nd Onset Temp. (°C)	2nd Endset Temp. (°C)	Peak Temp. (°C)		Residue After 600 °C (%)
					1st Peak	2nd Peak	
W0T0	273.69	490.39	--	--	469.66	--	1.32
W20T0	234.93	375.97	398.11	505.38	343.86	478.57	10.68
W40T0	228.19	383.52	397.69	504.89	348.85	479.66	12.96
W40T3	241.33	387.54	406.97	500.51	350.12	478.54	14.48
W40T6	235.28	381.88	396.89	504.35	353.58	477.06	16.97
W40T9	241.55	385.02	406.57	506.83	351.70	481.46	23.42

When Table 6 was examined, single-stage thermal degradation was observed in the control group without filler (W0T0) in the TGA analysis. Considering the values in Table 6, the decomposition for the W0T0 group started at approximately 273.7 °C and ended at approximately 490.7 °C. A similar result was reported by Esmizadeh *et al.* (2020). The maximum thermal degradation occurred at 469.7 °C for the W0T0 group samples, and the amount of residue after 600 °C was determined as 1.32%. If the W20T0 and W40T0 groups were examined, in which only wood flour was used as filler in different proportions, the thermal degradation occurred in two stages in the Derivative-TGA (drTGA) graphs in these groups, and two peaks were obtained on the graph (Fig. 4).

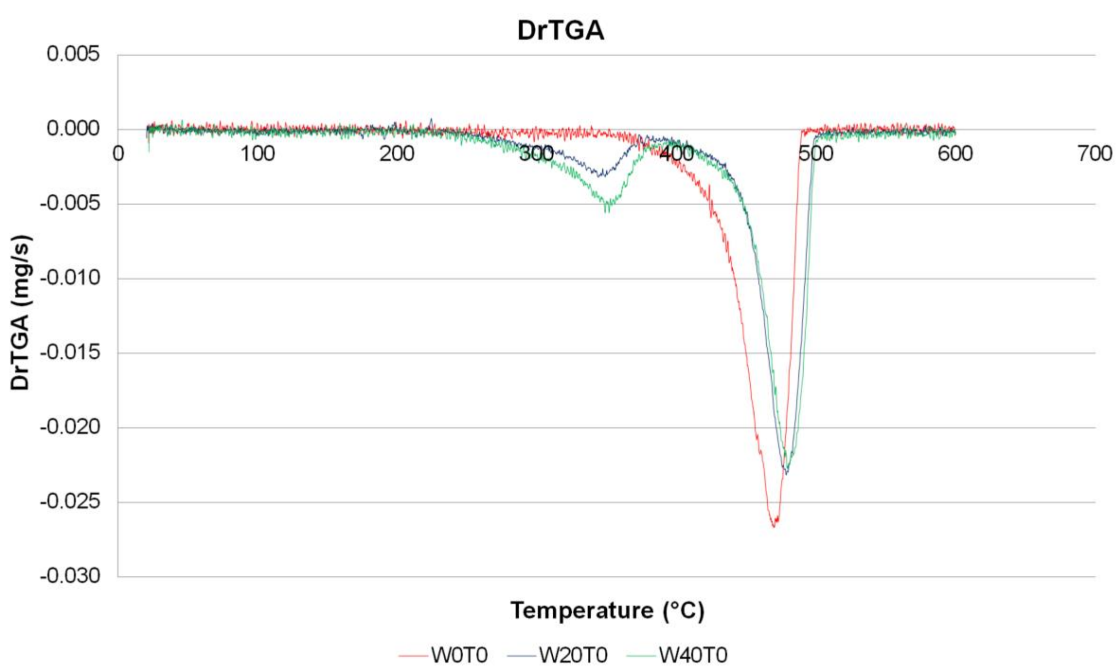

Fig. 4. DrTGA results of just WF reinforced PP-based composites

Considering the first peaks obtained in the DrTGA graphs in Fig. 4, the first decompositions were at 234.9 and 228.2 °C for W20T0 and W40T0, respectively. The first decomposition end-temperatures were approximately 376.0 and 383.5 °C, respectively. These first peaks formed because of the wood flours main components, cellulose, hemicellulose, and lignin in the WPCs. While the thermal degradation range of hemicelluloses was between 190 and 410 °C (Chen *et al.* 2020), for celluloses it was between 250 and 400 °C (Várhegyi *et al.* 1994). It is reported that lignin has a wider thermal degradation temperature range (between 105 and 800 °C) (Chen *et al.* 2020; Foong *et al.* 2020). Maximal degradation was observed at 343.9 °C with a 12.3% extent and at 348.9 °C with a 17.3% extent for the W20T0 and W40T0 groups, respectively. The degradation temperatures of WPCs produced by adding wood flour to the polymer matrix decreased. This occurred because wood flour started to decompose before the polymer matrix. The second degradation began at 398.1 and 397.7 °C and finished at 505.4 and 504.9 °C for W20T0 and W40T0, respectively. Maximal degradation was determined at 478.6 and 479.7 °C for W20T0 and W40T0, respectively. With the addition of wood flour, the maximum decomposition temperatures increased by approximately 10 °C compared to the control group. Considering the remaining residue amounts at 600 °C, the amount of residue also increased with the usage of wood flour compared to the control group. Furthermore, the increase in this residue amount continued with the increase in wood flour usage.

The thermal properties of WPC groups containing wood flour at the highest rate and TiO_2 at different levels were determined to observe the effects of TiO_2 on the thermal properties of WPCs. DrTGA graphs of WPCs groups containing 40% wood flour and different amounts of TiO_2 are given in Fig. 5.

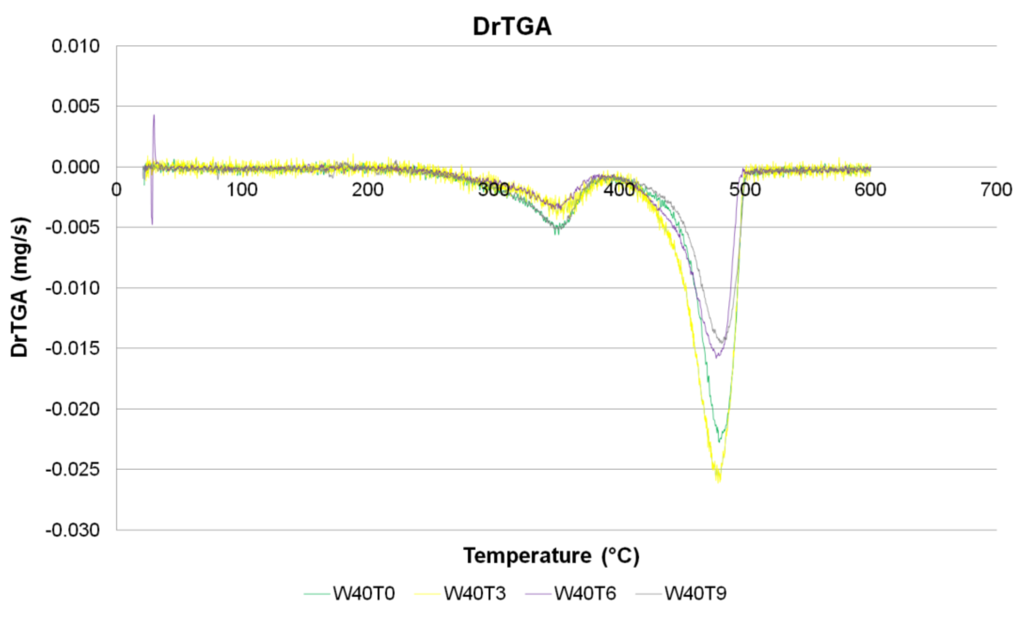

Fig. 5. DrTGA results of PP-based composites contain 40% WF and different amounts of TiO_2

From Fig. 5, it can be seen that the WPCs decomposed in two stages, and generally, close peaks were obtained. It was observed that the starting and ending temperatures of the peaks obtained in the groups in which the nanomaterial was used were close to each other. An increment was observed in the initial decomposition temperature with the usage of

TiO_2, and it was approximately 15 to 20 °C. The maximum thermal degradation temperature was determined at 350 °C for the first peak and at 479 °C for the second peak. The increment in the amount of TiO_2 in the WPCs also caused an increase in the amount of residue at 600 °C. In the W40T9 (23.42% residue at 600 °C) group, which contained the maximum amount of wood flour and nanomaterials, the amount of residue at 600 °C increased almost twice that compared to the W40T0 group (12.96% residue at 600 °C), which contained only 40% wood flour and without nanomaterial. In previous studies, it was stated that the decomposition for pure TiO_2 started at 200 °C and continued up to 950 °C (Özbey 2018). It is thought that the thermal stability of TiO_2 is higher than wood flour and that it wraps around the wood during its usage at high levels, which is caused by slowing down the degradation and decreasing the mass loss (%). In addition, it was reported that the thermal stability of the nanocomposite increased with the usage of nanoparticles in the lignocellulosic matrix (Rahman *et al.* 2017) and WPCs (Kaymakci 2019).

The DSC analyses were performed on eight different groups (W0T0, W20T0, W20T3, W20T6, W40T0, W40T3, W40T6, and W40T9). The crystallinity ratios of WPCs were calculated with the help of Eq. 1, which is presented in the "Methods" section, and are summarized in Table 7.

Table 7. DSC Results of WF and TiO_2 Reinforced PP-based Composites

ID	(1-α) (%)	T_m (°C)	ΔH_m (J/g)	ΔH_c (saf PP)(J/g)	X_c (%)
W0T0	97	161.5	129.6	207	64.53
W20T0	77	161.2	74.2	207	46.57
W20T3	74	160.7	67.1	207	43.80
W20T6	71	161.4	54.6	207	37.14
W40T0	57	160.2	43.3	207	36.72
W40T3	54	160.7	41.1	207	36.73
W40T6	51	161.1	40.6	207	38.42
W40T9	48	160.3	35.7	207	35.88

(1-α) is the weight fraction of polymer into the composite material, T_m is the melting temperature, X_c (%) is the crystallinity value, ΔH_m is the melting enthalpy of the specimens, and ΔH_c is the enthalpy value of melting of a 100% crystalline form of PP

Table 7 shows there was no significant change in melting temperatures, and they were close to each other. However, when the crystallinity ratio of the composites is examined, the crystallinity of the composites decreased with increasing amount of fillers to the polymer. While the melting temperatures of the composites did not change, decreases were determined in the crystallinity ratios (X_c) compared to the control group without filler (W0T0). While both fillers tended to decrease the crystallinity of the polymer, it is possible to say that wood flour loading reduced the crystallinity of the composites at a higher amount than TiO_2 loading with the results of the DSC analysis. While the highest crystallinity (X_c) ratio was determined in W0T0, containing just the coupling agent and lubricant, the lowest value was determined in the W40T9 group containing the maximum amount of both fillers.

Tribological Properties of WPCs

Generally, the tribological properties are described with the friction coefficient (CoF) and the specific wear rate (WR) (Tai *et al.* 2012; Hou *et al.* 2018; Yetgin 2020). Tribological tests of Iroko wood flour and TiO_2 filled PP-based WPCs were conducted under two different loads (30 and 60 N) at one sliding speed (1.0 m/s). The WRs calculated with Eq. 2 and the CoF values of the composites are presented in Table 8.

Table 8. Results of Friction Coefficient and Wear Rate of WPCs

ID	Load (N)		Load (N)	
	30	60	30	60
	Coefficient of Friction (μ)		Wear Rate (m^2/N)	
W0T0	0.314	0.369	2.576E-13	3.546E-14
W0T3	0.297	0.356	1.364E-13	8.112E-14
W0T6	0.281	0.332	2.925E-13	1.553E-13
W0T9	0.263	0.304	4.105E-13	1.088E-13
W20T0	0.275	0.354	1.089E-14	1.816E-14
W40T0	0.263	0.325	3.067E-14	5.112E-15
W40T3	0.302	0.406	6.479E-15	1.782E-14
W40T6	0.289	0.340	9.560E-15	9.560E-15
W40T9	0.275	0.320	1.239E-14	9.294E-15

In Fig. 6, the changes in CoF of neat PP polymer and wood flour and TiO_2-filled PP-based WPCs, depending on the applied load, are given. CoF values tended to decrease in composite groups that did not contain wood flour, and where TiO_2 was used as filler. CoF values decreased with the increase in the TiO_2 usage amount in these groups. Although there was an increase in CoF values of WPCs groups, which contained a level of 40% wood flour with the first loading of TiO_2 compared to the W40T0 group, CoF values decreased in the subsequent loadings of TiO_2. The CoF values in the WPC groups containing 40% wood flour at each subsequent TiO_2 loading exhibited a decreasing trend. The lowest CoF value was obtained in the W0T9 (just TiO_2 with maximum usage amount) and W40T0 (just wood flour with maximum usage amount) groups, which decreased approximately 16.2% compared to the neat PP. It is thought that the decrease in CoF values with the usage of TiO_2 is due to the self-lubrication properties of TiO_2. Birleanu *et al.* (2022) stated that TiO_2 is an up-and-coming lubricant filler for enhanced engine efficiency. Suryawanshia and Pattiwar (2018) added nano-TiO_2 into lubricating oil in their study. They reported that the CoF value was diminished approximately 6.1% in the group to which TiO_2 is added compared to the un-added group. A similar study was carried out by Rashed and Nabhan (2018). In that study, two different nanomaterials (TiO_2 and SiO_2) were added to engine lubricant oils, and the effects of these materials on the tribological properties of aluminum plates were investigated. They reported that while the best CoF values were obtained from 1 wt% of TiO_2-added mineral lubricant oils, whereas the best WR was with 1 wt% TiO_2-added semi-synthetic lubricant oils. However, they also stated that the addition of SiO_2 to engine oils did not have significant effects on the reduction of the friction coefficient (Rashed and Nabhan 2018).

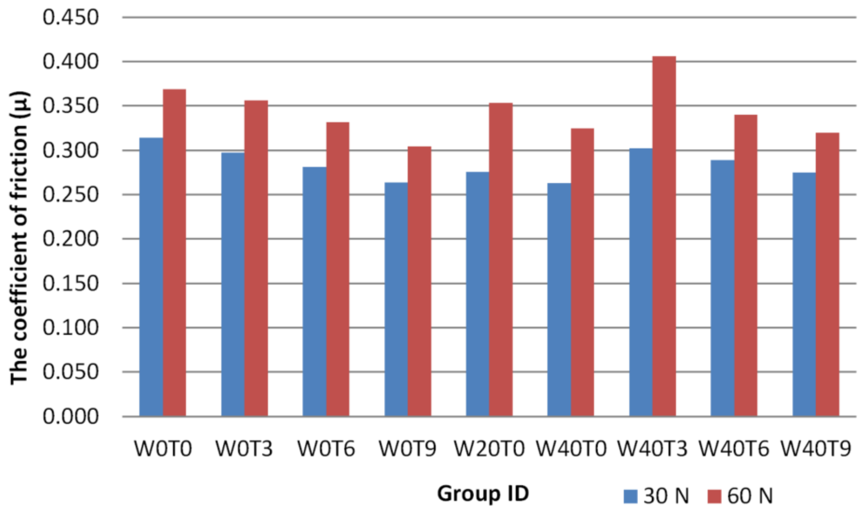

Fig. 6. The effect of fillers amount on WPCs friction coefficient

Figure 6 clearly shows that the CoF of WPCs was also decreased with the loading of wood flour. This reduction was obtained to the extent of 12.4% with the addition of 20% wood and approximately 16.2% with the addition of 40% wood flour. Although the CoF values slightly increased with the increase of the load from 30 to 60 N, the trend did not change, and the CoF of WPCs slightly decreased with the increasing amount of wood flour. Similar results were reported in a previous study (Aurrekoetxea *et al.* 2008). In the literature, the decrease in the CoF value can be attributed to the deterioration of the composite structure, the geometric structure of the composite, and the formation of the transfer film layer on the counter-disc (Samyn and Schoukens 2009). To show the effect of wood flour amount on CoF, counter-disc images of composites containing only wood flour in different amounts and the neat PP groups are given in Fig. 7.

When the disc images were examined in Fig. 7-a, individual and clumped wear residues were seen, and vaguely transferred film occurred in the neat PP group. Due to the intensive wear debris, the polymer did not plaster to the counter-disc, causing the light transfer film layer. Therefore, the light transfer film causes the COF to be higher than the groups that formed the intensive transfer film layer. When the disc images of the W20T0 (Fig. 7-b) and W40T0 (Fig. 7-c) groups containing wood flour (under 30 N load) were examined, it is seen that a transfer film layer was formed more intensely than the neat PP group, and less wear debris was present. These reduce the friction between the pin and the disc. The transfer film formation on the disc is thought to reduce the direct contact between the polymer matrix and the counter disc. Thus, this reduced the friction coefficient value of WPCs. Similar results were reported in the PP-based wood plastic study (Ibrahim *et al.* 2019). Yetgin (2020) stated that COF values decreased due to the transfer film formation on the disc in his study on determining the tribological properties of polymer composites. It has been noted that this causes the reduction of direct contact between the WPCs and the counter-disc. The COF slightly increased with increasing load. When the disc images of the samples applied with 60 N load are examined, it can be seen that the less of a transfer film layer formed in the control group (W0T0) (Fig. 7-d), which did not contain wood flour and TiO_2, but less residue was formed compared to the same group to which the 30 N load was applied, and these residues were clustered.

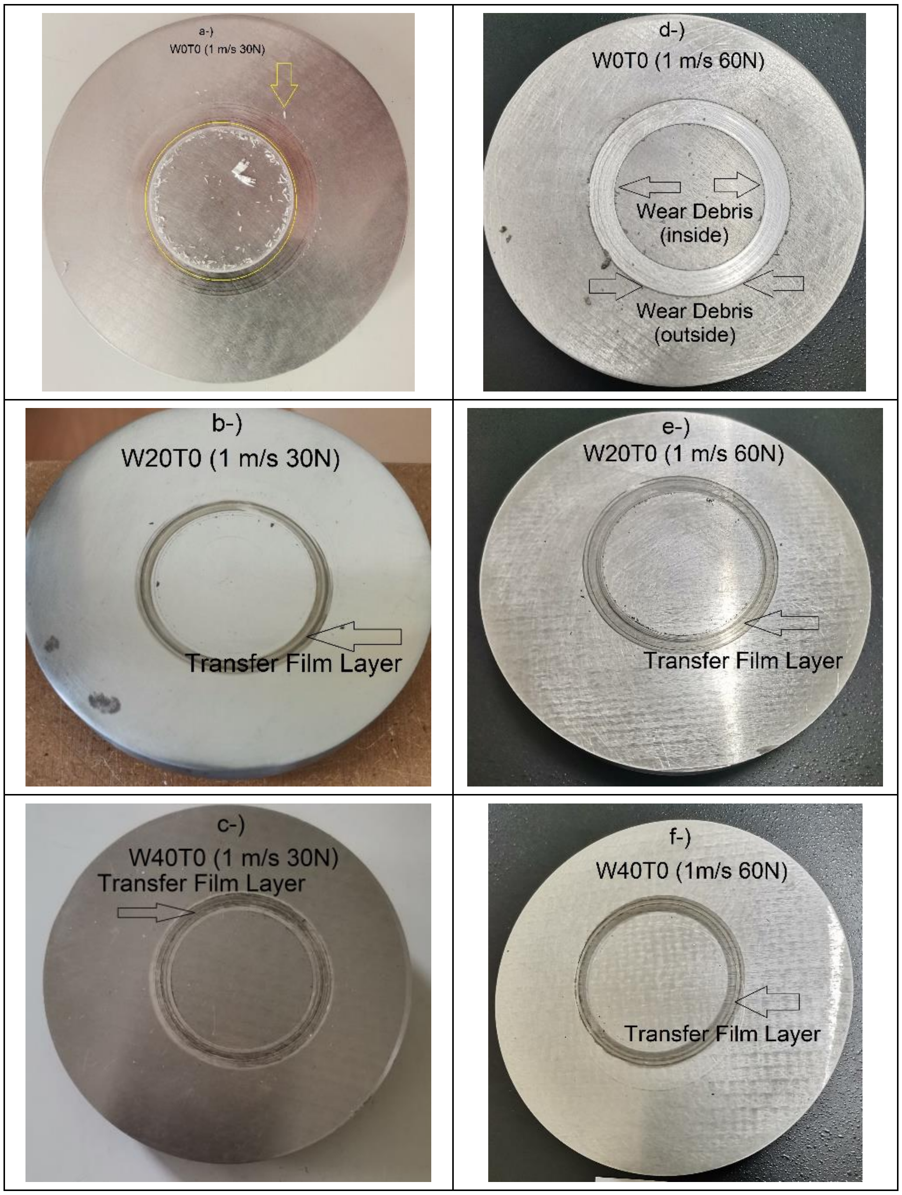

Fig. 7. Macro pictures of disc surface of neat PP and wood flour-filled groups: a-) W0T0 (30 N), b-) W20T0 (30 N), c-) W40T0 (30 N), d-) W0T0 (60 N), e-) W20T0 (60 N), and f-) W40T0 (60 N)

When the disc images in Fig. 7-e and Fig. 7-f are considered, it can be seen that a fainter and more transparent transfer film layer was formed than the images of the same groups under 30 N loads. In addition, it is understood that less residue is formed on the counter-disc from these images. Less residues on the disc decreased the WR with the increase in the load based on the related Eq. 2. Furthermore, the density values of WPCs increased with the addition of wood flour and TiO_2. Based on the same equation, the increase in density of WPCs and load also reduced the WR with fewer residues. Moreover, it can be seen from the images in Fig. 7 that the transfer film layers plastered more effectively on the counter-disc surface with the increase of the applied load.

The effect of filler levels on WPCs WR is given in Fig. 8. It can be seen from the graph that the WR sharply decreased with the first loading of the wood flours under the 30 N load. A slight increase was observed in the subsequent wood flour loading under the same load. Under 60 N load, WR values tended to decrease with each wood flour loading amount. In general, the WR values of WPC groups, in which TiO_2 is employed alone as filler, tended to increase with the rise in the amount of usage. In addition, the WR values significantly decreased with the increase in the applied load in these WPC groups. However, a synergetic effect occurred on the wear properties of WPCs with the usage of both fillers together.

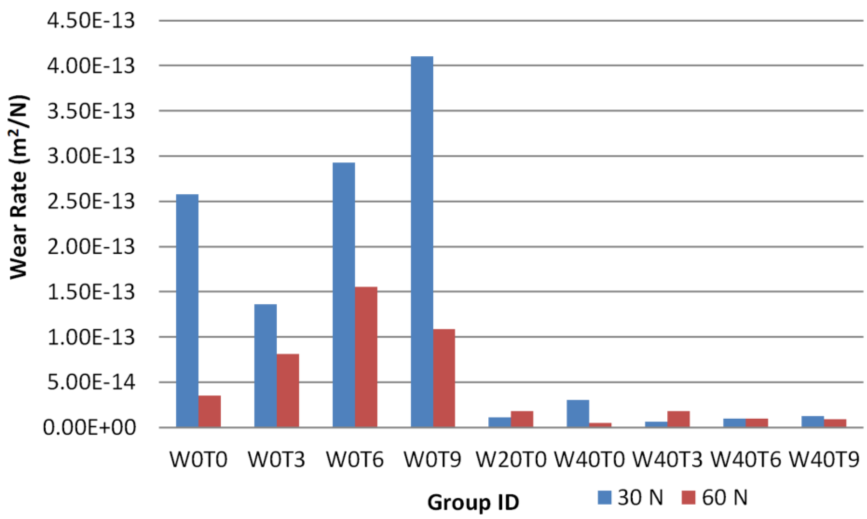

Fig. 8. The effect of fillers amount on WPCs wear rate

Mechanical Properties of WPCs

The variation ratios of WPC properties determined with the help of the related Eqs. 3 through 5 are given in Table 9. Values with a plus sign indicate an increase in the relevant properties after weathering, and values with a minus sign indicate a decrease after weathering. The mechanical (before and after the weathering) properties of WPCs are summarized in Table 10.

Table 9. Variation Ratios of Mechanical Results of the WPCs

Group No.	TS (%)	EatB (%)	FS (%)	MOE (%)	IS (%)
W0T0	-16.6	-98.9	+8.5	+44.9	-46.3
W0T3	+0.9	-90.9	+7.8	+7.1	+1.6
W0T6	-0.3	-94.4	+7.1	+7.9	-5.1
W0T9	+5.9	-96.4	+1.2	+1.0	+0.2
W20T0	-11.7	-13.3	-6.6	-6.4	-15.2
W20T3	-2.2	-10.7	-3.8	-0.4	-8.2
W20T6	-5.9	-2.0	-2.1	+1.4	+2.2
W20T9	-5.1	-6.1	+7.7	+12.9	-1.9
W40T0	-7.2	-9.5	-6.9	+0.3	-0.2
W40T3	-5.5	-5.4	-5.0	+1.3	+4.4
W40T6	+3.2	-4.1	+9.6	+22.3	-2.1
W40T9	-5.6	-4.0	+6.5	+11.1	+3.0

Table 10. Summary of Mechanical Results of the WPCs

Group No.	TS (MPa)		EatB (%)		FS (MPa)		MOE (MPa)		IS (Kj/m^2)	
	Before	After	Before	After	Before	After	Before	After	Before	After
W0T0	26.59 (0.44)*	22.19 (1.29)	362.63 (7.57)	4.11 (0.45)	31.21 (1.15)	33.86 (0.87)	911.51 (29.58)	1320.35 (138.23)	3.21 (0.28)	1.73 (0.18)
W0T3	28.21 (0.57)	28.48 (0.31)	346.22 (9.34)	31.39 (6.00)	36.18 (1.34)	39.00 (2.86)	1137.34 (41.20)	1217.92 (88.23)	2.68 (0.12)	2.73 (0.18)
W0T6	29.95 (0.51)	29.86 (0.98)	338.34 (5.64)	18.83 (3.32)	39.37 (0.85)	42.16 (1.91)	1257.19 (26.56)	1356.49 (63.33)	2.68 (0.07)	2.54 (0.10)
W0T9	30.11 (0.13)	31.90 (0.62)	325.79 (5.62)	11.60 (0.98)	39.70 (0.61)	40.19 (1.56)	1274.13 (22.59)	1286.31 (39.87)	2.89 (0.13)	2.90 (0.09)
W20T0	26.54 (1.12)	23.43 (0.26)	4.61 (0.30)	4.00 (0.19)	47.51 (0.77)	44.38 (3.13)	2132.57 (33.02)	1996.43 (190.99)	3.45 (0.30)	2.92 (0.37)
W20T3	27.13 (0.95)	26.54 (1.14)	4.55 (0.19)	4.06 (0.31)	48.50 (1.45)	46.67 (0.85)	2196.22 (69.65)	2187.74 (100.36)	3.21 (0.19)	2.95 (0.24)
W20T6	27.81 (0.68)	26.16 (1.28)	4.34 (0.12)	4.25 (0.07)	48.77 (1.09)	47.77 (1.05)	2256.46 (79.72)	2286.98 (25.32)	3.14 (0.12)	3.21 (0.23)
W20T9	28.38 (1.22)	26.93 (0.51)	4.38 (0.20)	4.11 (0.13)	49.13 (1.12)	52.93 (1.57)	2321.24 (51.95)	2620.64 (69.55)	3.19 (0.09)	3.13 (0.29)
W40T0	27.46 (0.61)	25.49 (1.25)	3.20 (0.27)	2.90 (0.17)	49.01 (1.20)	45.62 (1.62)	3046.10 (74.99)	3053.85 (95.87)	3.83 (0.38)	3.82 (0.30)
W40T3	27.91 (0.41)	26.39 (1.17)	3.00 (0.18)	2.84 (0.14)	50.92 (1.64)	48.39 (1.37)	3373.64 (198.07)	3418.05 (133.05)	3.81 (0.25)	3.98 (0.22)
W40T6	26.08 (0.99)	26.93 (0.47)	2.94 (0.05)	2.82 (0.12)	46.92 (1.79)	51.40 (2.40)	3102.92 (126.13)	3795.57 (185.28)	3.58 (0.31)	3.51 (0.16)
W40T9	27.58 (1.01)	26.04 (0.54)	2.70 (0.07)	2.59 (0.15)	46.05 (2.68)	49.04 (1.99)	3429.02 (124.76)	3810.96 (182.26)	3.48 (0.10)	3.59 (0.24)

*The numerical value in the parenthesis is standard deviation. Ts: Tensile strength, EatB: Elongation at break, FS: Flexural strength, MOE: Flexural modulus, IS: Impact strength. 'Before' refers to the average strength and modulus values measured before weathering. 'After' refers to the average strength and modulus values measured after weathering.

Interaction graphs examining the effects of fillers on tensile strength properties are presented in Fig. 9.

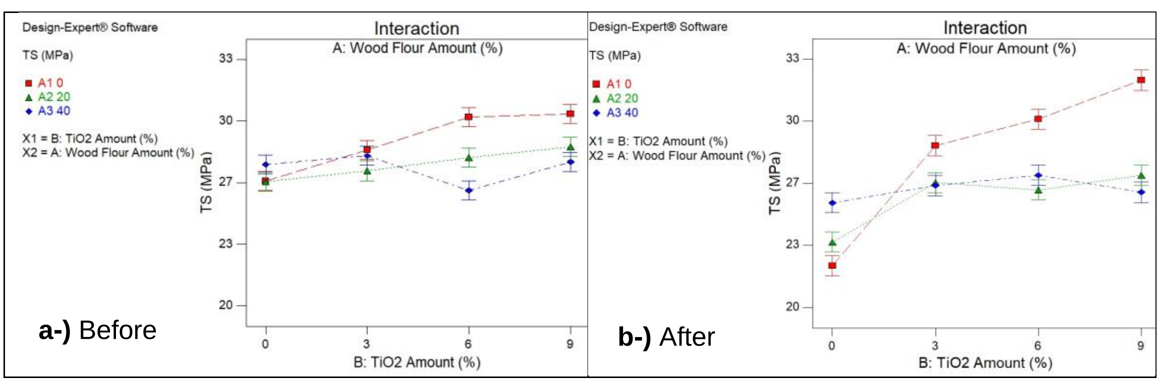

Fig. 9. The effects of fillers amount on tensile strength of WPCs; a-) Before weathering, b-) After weathering

When the interaction graph of the tensile strength (before weathering) in Fig. 9-a was examined, it was determined that both fillers had a statistically significant effect on the tensile strength values ($P < 0.0001$). The tensile strength values were preserved with the first addition level of lignocellulosic filler, and similar results to the neat PP group were obtained.

A slight increase in tensile strength was observed using Iroko flour at a 40% level. The MAPP was utilized as a coupling agent in the formulation to obtain better adhesion between wood and polymer, and this might lead to enhancement in the tensile strength. The well-known way is the usage of MAPP and MAPE as coupling agents to increase interaction and improve the adhesion between the hydrophobic polymer matrix and hydrophilic lignocellulosic material (Ismail *et al.* 2002; Annie Paul *et al.* 2008; Mengeloğlu and Karakuş 2008; Nourbakhsh and Ashori 2008; Rao *et al.* 2018; Başboğa *et al.* 2020). Compatibilization of wood flour improved its dispersion in the polymer matrix and provided better adhesion to a polymer resulting in increased tensile strength. Similar results were reported by Ramezani Kakroodi *et al.* (2013) and Woodhams *et al.* (1993). The tensile strength properties were improved with the addition of TiO_2 in the matrix in the groups that did not contain wood flour and also contained 20% wood flour. The tensile strength values also increased with the increase of the nanomaterial incorporation level. Although slight fluctuations were observed in the tensile strength values in the groups where wood flour was used at the maximum amount (40%), results were generally obtained within the close ranges. These fluctuations are thought to be caused by the formation of agglomerates due to the high usage of fillers. Similar results have been reported, especially in the study using nano TiO_2 at a 5% level (Ghalehno *et al.* 2020). Achieving uniform distribution with a high usage amount of nanoparticles is difficult because of their high surface energy. The nanoparticles have a high tendency for agglomeration (Rong *et al.* 2006). Kord *et al.* stated that nanoparticles show better distribution when they are used at lower concentrations. In addition, Kord *et al.* also underlined that high usage amounts of nanoparticles cause a decrease in the mechanical properties of composite materials due to their higher agglomeration (Kord *et al.* 2011). In general, the usage of TiO_2 positively affected the tensile strength values. It is thought that this increase is because of the higher contact surface between the polymer matrix and the particles obtained with the usage of nano TiO_2 with a higher surface area. Similar results were obtained by others (Hazarika and Maji 2013; Kaymakci 2019; Ghalehno *et al.* 2020). Kaymakçı (2019) stated that this improvement was because the composites that contained TiO_2 had a harder structure than the groups that did not contact the mineral particles.

When the tensile strength of the samples after weathering is examined, it can be observed that the usage amounts of both fillers and the amount of filler had significant effects on the tensile strength values ($P < 0.0001$). Furthermore, it was determined that weathering also significantly affected tensile strength properties ($P < 0.0001$). The effects of weathering on the tensile strength properties of WPCs decreased with the usage of wood flour as filler. A decrease in the mechanical strength values of composites after weathering is expected (Stark and Matuana 2007). Exposure of polymers to UV radiation causes cleavage of polymer chains and, thus, photo-oxidative degradation. This leads to the emergence of free radicals, molecular weight loss, and mechanical strength reductions (Stark 2007; Yousif and Haddad 2013). It was thought that the usage of Iroko wood flour tolerated the deterioration effect of weathering factors on the tensile strength of WPCs. Similar results were recorded in the literature (Boran Torun *et al.* 2021). In the groups using TiO_2 as filler, better protection from weathering effects was achieved compared to those using wood flour. In the groups where only TiO_2 was used as filler, the tensile strength values after weathering were either preserved or better results were obtained than the values before weathering. In these groups, an improvement was achieved in the changing rate in the tensile strength values after weathering with the increase in TiO_2 usage amount. In the groups where TiO_2 was used together with wood flour, the effects of weathering on the tensile strength decreased with the presence of TiO_2 in the matrix, but this protection was provided up to 6% of usage, and it was observed that there was no significant change in tensile strength values after weathering when used at a higher addition level. While the highest decrease in tensile strength values after weathering was obtained in the neat PP group without any filler, the best result was obtained in the W0T9 group, where only 9% of TiO_2 was used as filler, with +5.9% improvements. The results obtained are compatible with similar studies in the literature (Hazarika and Maji 2013; Çavuş 2017). Hazarika and Maji (2013) stated that the effect of UV radiation on tensile strength decreased with the increase in the amount of TiO_2 usage, and this was due to the UV protection effect provided by TiO_2.

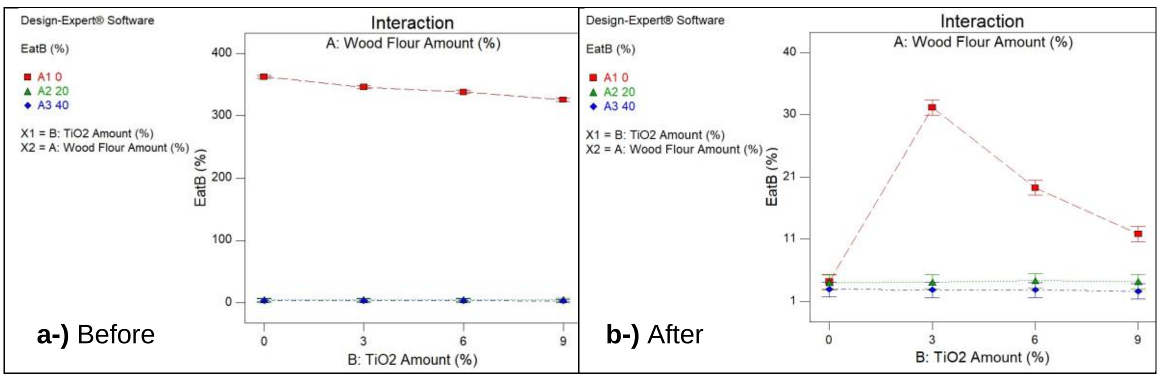

Fig. 10. The effects of fillers amount on elongation at break properties of WPCs: a-) Before weathering, b-) After weathering

For elongation at break (EatB) properties, it has been determined that wood flour and TiO_2 usage amounts were significantly effective relative to the EatB values of weathered and un-weathered composites ($P < 0.0001$). The usage of wood flour significantly reduced the EatB values of the WPCs before weathering. When the percentage of lignocellulosic filler loading was enhanced, the smoothness and ductility of the polypropylene matrix were greatly diminished. Usually, the usage of natural filler in composites provides lower EatB values and a higher modulus (Sain and Panthapulakkal 2006). The use of TiO_2 also slightly reduced the EatB values of the WPCs before weathering. In the literature, it has been stated that an increase in the WPCs hardness values causes a decrease in the EatB values (Yam *et al.* 1990; Clemons 2002; Sain and Panthapulakkal 2006; Çavuş 2017). Similar to tensile strength, it has been observed that weathering has a significant effect on EatB values. It is seen from the interaction graph in Fig. 10-a that wood flour was more effective relative to the EatB values compared to TiO_2. However, the highest decrease in the EatB values after weathering was observed in the control and composite groups that did not contain wood flour but only TiO_2. Nevertheless, the highest EatB values after weathering were determined in composite groups containing only TiO_2. Similar results were presented by others (Çavuş 2017).

Interaction graphs showing the effects of fillers on FS are presented in Fig. 11. Results showed that the FS (before and after weathering) were significantly affected by both fillers (P < 0.0001). First, the flexural strength properties of WPCs before weathering are examined; it was seen from Fig. 11-a that a clear increment in FS values was obtained with the first loading of the wood flour. A slight increase in FS values was observed at the next loading level of 40%. It is thought that the polymer is thoroughly wrapped around the wood, and thus, the effective load transfer occurred between the wood fibers, which have higher flexural strength than the neat polymer and polymer matrix. In this way, it is thought that the flexural strength values of wood-filled PP-based composites were increased. In previous studies in which different lignocellulosic materials were used as fillers, an increment in the flexural strength values was observed with the increase in the amount of lignocellulosic filler (Karmarkar *et al.* 2007; Yang *et al.* 2007; Yuan *et al.* 2008; Başboğa *et al.* 2020).

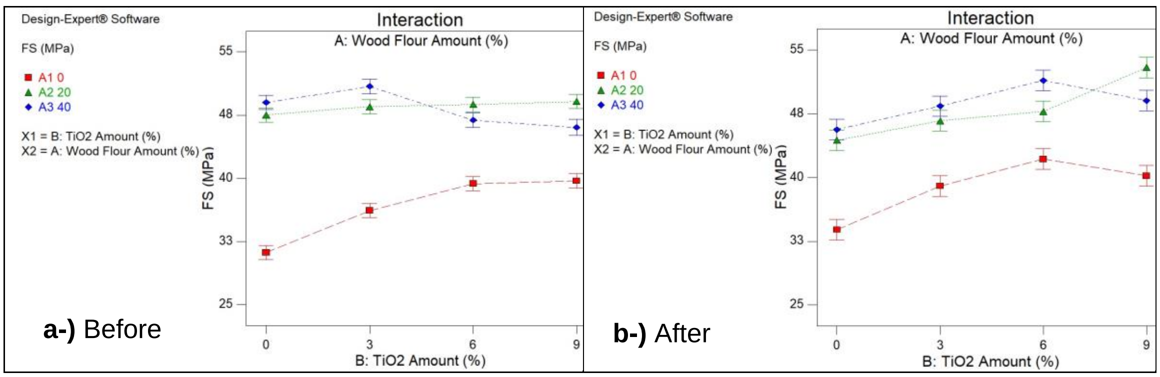

Fig. 11. The effects of fillers amount on flexural strength of WPCs: a-) Before weathering, b-) After weathering

When the effects of TiO_2 on the flexural strength values of composites are examined, the flexural strength values of the composites are increased with increasing amount of TiO_2. Han *et al.* (2008) explained this by the fact that nanoparticles fill the gaps between composite components and thus improve mechanical strength values. Deka and Maji (2011) stressed that the uniform distribution of TiO_2 nanoparticles and clay nanoparticles increased composites' flexural and tensile properties. Different researchers have observed similar results (Saeed *et al.* 2009; Aydemir *et al.* 2016; Wang *et al.* 2020). However, the trend of increased flexural strength values decreased with the maximum level usage amount of the TiO_2. In the composite groups that do not contain wood flour, the flexural strength values increased approximately 6.1% compared to the neat PP group (W0T0) using 3% of TiO_2 (W0T3). In the W0T6 group, which contained 6% of TiO_2, an increase of 6.2% was observed compared to the W0T3 group. In the W0T9 group, which contained a maximum level of TiO_2, an increase of 0.5% was obtained compared to the W0T6 group. It is thought that this is due to the increase in regional agglomeration, especially with the usage of TiO_2 above 6%. The SEM images in Fig. 2-c/d support the agglomeration of TiO_2 nanoparticles. Previous studies reported similar results (Ashori and Nourbakhsh 2011; Deka and Maji 2011; Ghalehno *et al.* 2020).

The weathering process significantly affected the flexural strength properties (P = 0.0407). When the flexural strength properties of WPCs after weathering are examined (Fig. 11-b), parallel results to the FS obtained before weathering were observed. In addition, the effects of both fillers on FS were observed in parallel with the effects before weathering. WPCs containing just TiO_2 and neat PP showed an increment in the FS values after weathering. Weathering effects on FS properties were reduced in all WPC groups by using TiO_2 up to 6%. With the usage of TiO_2, either improvement was achieved in FS values or the decrease in FS values was reduced. This was due to the UV protection effect provided by TiO_2 (Hazarika and Maji 2013). Furthermore, the highest improvement in FS values after weathering was obtained in the W40T6 group with 9.6%. In addition, the next highest improvements were achieved in the neat PP, W0T3, W20T9, and W0T6 groups with 8.5%, 7.8%, 7.7%, and 7.1%, respectively. In addition, ASTM D6662 (2001) standard requires a minimum flexural strength of 6.9 MPa (1000 psi) for polyolefin-based plastic lumber decking boards. In this study, all composite groups (before and after weathering) provided flexural strength values (31.21 to 52.93 MPa) that were well over the requirement by the standard (ASTM D6662 2001).

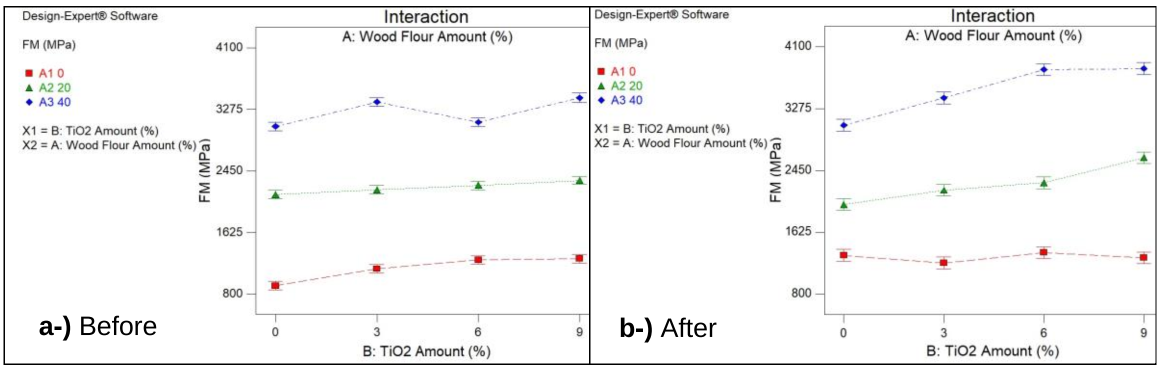

Fig. 12. The effects of fillers amount on flexural modulus (MOE) of WPCs; a-) Before weathering, b-) After weathering

The interaction graphs for the flexural modulus (MOE) (before and after weathering) of composites are presented in Fig. 12. It was determined that the weathering process and both fillers had a significant effect on the MOE values (before and after weathering) ($P < 0.0001$). However, from the interaction graphs in Figs. 12-a and 12-b, it can be clearly seen that wood flours had a higher effect on MOE values than TiO_2. MOE values were increased with the increment of wood flour amounts. Similar results were also reported for other wood flours-filled polymer composites (Woodhams *et al.* 1993; Wang *et al.* 2003; Mengeloglu *et al.* 2007; Santiagoo *et al.* 2011; Ramezani Kakroodi *et al.* 2013; Pang and Ismail 2014). Lignocellulosic fillers show a higher modulus compared to polymers. This is one of the advantages of lignocellulosic fillers over polymers. That advantage leads to a higher modulus for WPCs than neat polymers (Ismail *et al.* 2002). Before weathering, MOE values were slightly increased with the loading of TiO_2. The MOE results support the hardness values. Both fillers increased the hardness values of the WPCs. The WPCs became harder, and that means they had a harder structure. Hence, it can be said that this harder structure caused an increase in the MOE. MOE values of all WPCs increased after weathering except W20T0 and W20T3 groups. After weathering, a 6.4% decrease was determined in the MOE values of the W20T0 group, while a negligible decrease was determined in the W20T3 groups (0.4%). TiO_2 effects on MOE properties of WPCs containing wood flours were more prominent after weathering. The biggest improvement in MOE values was observed in neat PP (44.9%), W40T6 (22.3%), and W40T9 (11.1%) groups, respectively. The variation of MOE values decreased with the increased filler amounts. Cross-linking and chain scission can occur in polyolefins with the

UV radiation effects during weathering, leading to obvious differences in the crystallinity of composites. Lee *et al.* (2012) claimed that the crystallinity of PP and recycled-PP-based WPC increased after 1000 h accelerated UV weathering application at 72.3% and 165.9%, respectively (Lee *et al.* 2012). In a similar study about the PP-based WPCs, it was stated that the crystallinity of PP increased with prolonged exposure to weathering (Fabiyi and McDonald 2014). It is known that a secondary crystallization in polyolefins occurs at the early stage of the degradation under the UV radiation effects, leading to the increment of the MOE of the polyolefin-based composites (Stark and Matuana 2007; Hung *et al.* 2012; Badji *et al.* 2017; Boran Torun *et al.* 2021). Through PP recrystallization, short PP chains accumulate and form crystalline regions that should benefit from flexural properties (Peng *et al.* 2014). ASTM D6662 (2001) standard requires a minimum flexural modulus of 340 MPa (50,000 psi) for polyolefin-based plastic lumber decking boards. In this study, W0T0 (before weathering) group provided minimum MOE values of 912 MPa, while W40T9 (after weathering) group provided maximum MOE values of 3810 MPa. These values are well over the required standards.

The effects of fillers on the notched impact strength (IS) properties of WPCs are given in Fig. 13.

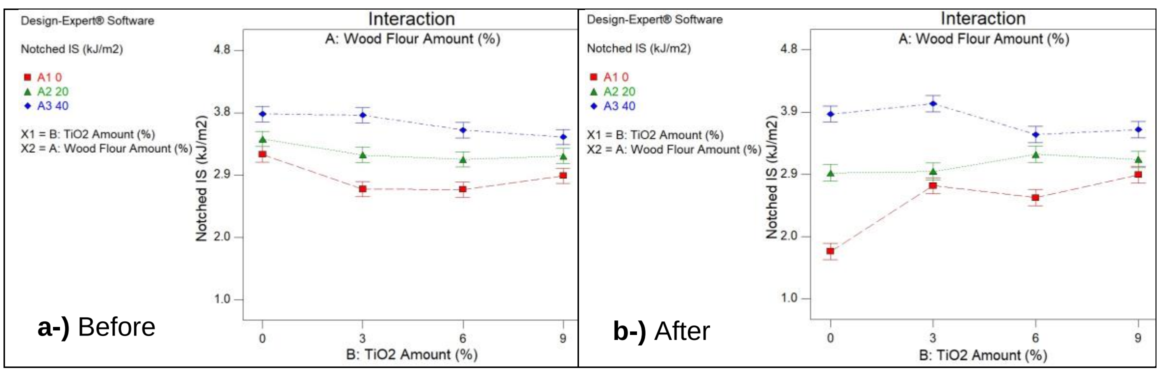

Fig. 13. The effects of fillers amount on notched impact strength of WPCs; a-) Before weathering, b-) After weathering

The effects of fillers on the IS properties of WPCs before weathering are presented in Fig. 13-a. Wood flours and TiO_2 usage amounts were significantly effective relative to IS properties of WPCs ($P < 0.0001$). While the IS properties of WPCs were positively affected by the usage of wood flour, the usage of TiO_2 had a negative effect. With 20% wood flour usage, IS values increased 7.5% compared to neat PP, while IS values rose 19.3% with wood flour usage at the maximum level. While describing the flexural strength properties, it is thought that the polymer is thoroughly wrapped around the wood, and thus leads to an increment in the interaction between polymer matrix and wood flours. The effective load transfer occurred between the wood fibers and polymer matrix through the better adhesion between polymer blends and wood flours. Yuan *et al.* (2008) stated that the IS values increased with the wood flour content in the groups where MAPP was utilized as a coupling agent in WPC production. Additionally, they attributed this increase to the fact that more energy is required to break the wood fiber during breakage. In IS values, an increment of until 40% was observed in WPC groups using MAPP and with 50% wood flour content compared to neat PP (Yuan *et al.* 2008). Furthermore, Burgada *et al.* (2021) also reported similar results, and they attributed the ability of the materials to dissipate energy when pulling the fibers away from the polymer matrix. Hence, it is thought that the IS values of wood-filled PP-based composites were increased. Saeed *et al.* (2018) stated that 5% of maleic anhydride grafted high-density polyethylene (MA-HDPE) was used as a coupling agent, and the IS values increased approximately 10 to 12%. They concluded that this might be due to the increase in the adhesion between polymer blends and wood flour. They stated that the impact strength of Poly(butylene succinate) (PBS)/Poly(lactic acid) (PLA)/Wood flour (WF)/MA-HDPE blends is improved due to better adhesion between polymer blends and WF bonding. Moreover, they stated that a tougher structure was formed in WPCs with the usage of MA-HDPE (Saeed *et al.* 2018). Wu *et al.* (2020) utilized tung oil anhydride (TOA) as a compatibilizer in the manufacturing of hemp fiber-filled PP-based WPCs. Twice higher IS values were obtained in the lignocellulosic-filled group using compatibilizer compared to the group without compatibilizer (Wu *et al.* 2020). Similar results were reported by others (Lu and Oza 2013). A 16.5% decrease in IS values was determined with the first 3% use of TiO_2. In the W0T6 group, with the subsequent addition of 3% TiO_2, the same average IS value was obtained as the W0T3 group. In contrast, the IS values of the W0T9 group, in which TiO_2 was used at the maximum level, increased 7.8% compared to the W0T3 and W0T6 groups but decreased 10% compared to the neat PP. In the usage of TiO_2 with wood flours, a decreasing trend was observed in the IS values in general with the increase in TiO_2 usage amount. It is thought that the reason for the decrease in IS values due to the utilization of TiO_2 as a filler is that nanoparticles have limited the mobility of the polymer chains by filling even the smallest gaps between composite components. Contrary to the FS properties, filling these gaps caused a decrease in IS values.

The effects of weathering on IS properties of WPCs were significant ($P < 0.0001$). It was determined that the usage amounts of both fillers had a significant effect on the IS properties of WPCs obtained after weathering ($P < 0.0001$). Although there was a general decreasing trend in IS values with the effect of weathering, some WPC groups containing filler/s showed slight increases, up to a maximum of 4.4%. Moreover, the maximum reduction of IS values was obtained from the neat PP group. Among the next highest decrease in IS values, it was determined as 15.2% in the W20T0 group, which contains only 20% wood flour. The reduction in IS values of WPCs became negligible (0.2%) as the wood flour utilization level increased 40%. It was thought that the usage of wood flour tolerated the deterioration effect of weathering factors on the IS of WPCs. In the groups in which TiO_2 was used, either slight increases were observed or decreases were detected at a maximum of 5.1%. This is thought to be due to the UV protection effect provided by TiO_2 (Hazarika and Maji 2013).

Morphological Properties of WPCs

The SEM images of un-weathered WPCs presented in Fig. 14 were taken with an Everhart–Thornley detector (ETD) at 200 and 1000 magnifications. The SEM images taken with the Compositional Back-Scattered detector to support the presence of TiO_2 in WPCs containing 40% wood flour and different TiO_2 amounts are presented in Fig. 2. From Fig. 2-c-d, some small agglomerations were determined in some areas of fractured surfaces of WPCs containing nanomaterials at high levels, such as 6% and 9%. Especially, decreases or fluctuations were observed in the strength values of the groups in which wood flour was used at the highest amount, with TiO_2 at 6% and 9%.

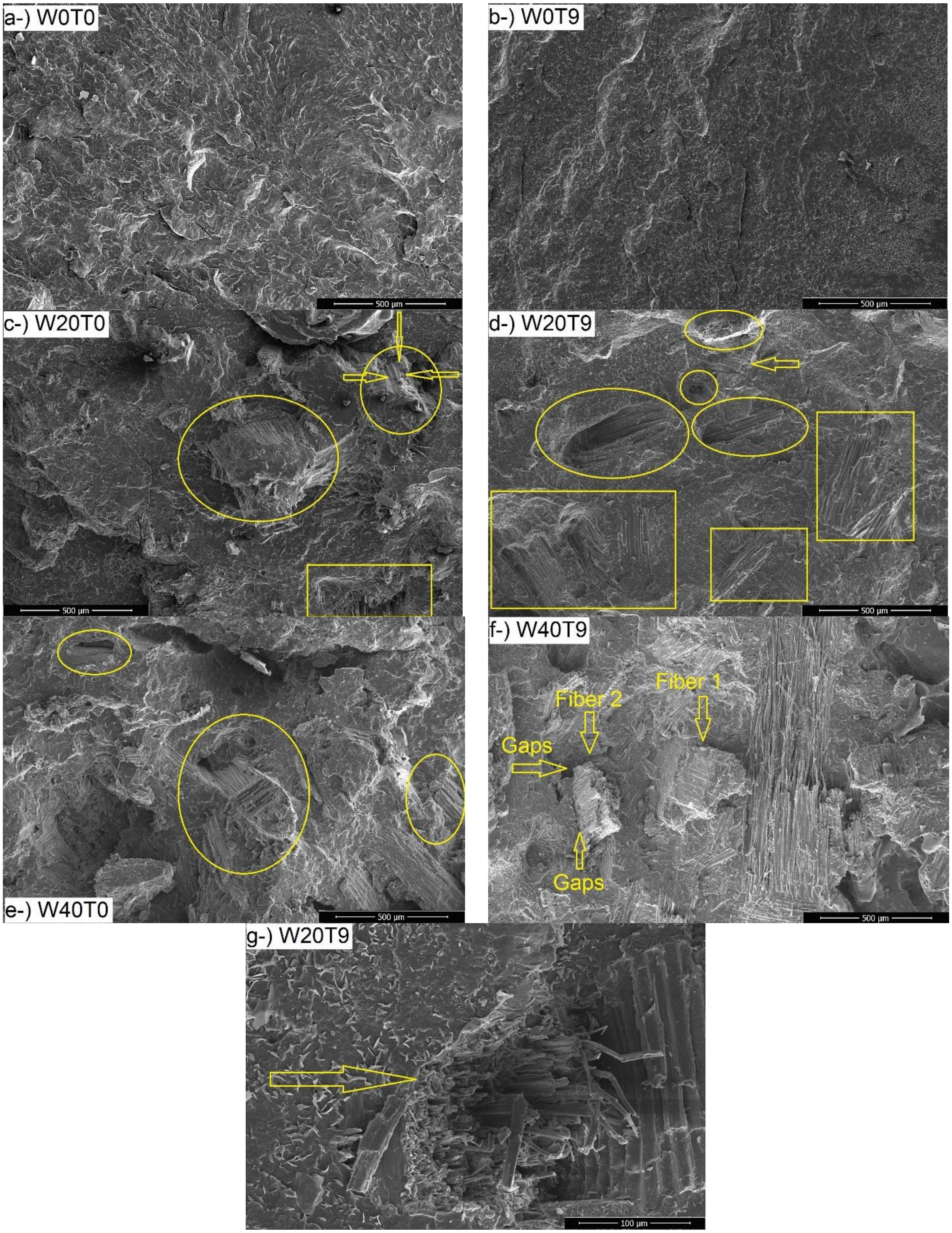

Fig. 14. SEM images (taken at 200 magnification, except g-) W20T0) of WPCs taken with a ETD detector; a-) W0T0, b-) W0T9, c-) W20T0, d-) W20T9, e-) W40T0, f-) W40T9, and g-) W20T9 (taken at 1000 magnification)

From the image in Fig. 14-f, while it is seen that Fiber 1 was completely wrapped by polymer and no hollow structure was formed, it is seen that there were gaps around Fiber 2 and between the polymer. It has been observed that gaps were formed between some fibers and polymer matrix by the usage of a high TiO_2 level, which led to a reduction of interaction between polymer and wood flour. This is thought to be why there were fluctuations in the values of the W40T6 and W40T9 groups in the strength interaction graphs. It was seen that the PP matrix was wrapped firmly around the wood flour particles, and it shows that the interface interaction was nevertheless robust even after the fracture of samples from images of WPCs containing only wood flours with 20% and 40% in Fig. 14-c and Fig. 14-e, respectively. When the SEM image of the W20T9 group taken at 1000 magnification in Fig. 14-g is examined, it can be seen that a part of the fiber in the matrix remained in the polymer after breaking the composite material, and the fibrils were fringed after breaking. From this image (Fig. 14-g), it can be said that the polymer tightly surrounds the fiber, and at the time of breakage, the fiber breaks without stripping. Additionally, these images may also help to explain the increment in strength values with increasing wood flour amounts in the polymer matrix. Furthermore, more stable results were obtained in the strength values of the groups containing 20% wood flour by changing the TiO_2 contents than the groups containing 40% wood flour. Figures 14-d, 14-f, and 14-g support these results.

Effect of Weathering on Color Changes of WPCs

The total color changes by accelerated weathering effects' measurements were recorded periodically at the same intervals (0, 24, 48, 72, 96, 120, 144, 168, 336, 504, and 672 h) on the surfaces of the samples exposed to UV degradation. Total color changes (ΔE) of WPCs were calculated using the related equation (Eq. 6). Graphs of quantified color changes in lightness (ΔL^*) and ΔE values are presented in Fig. 15 and Fig. 16, respectively.

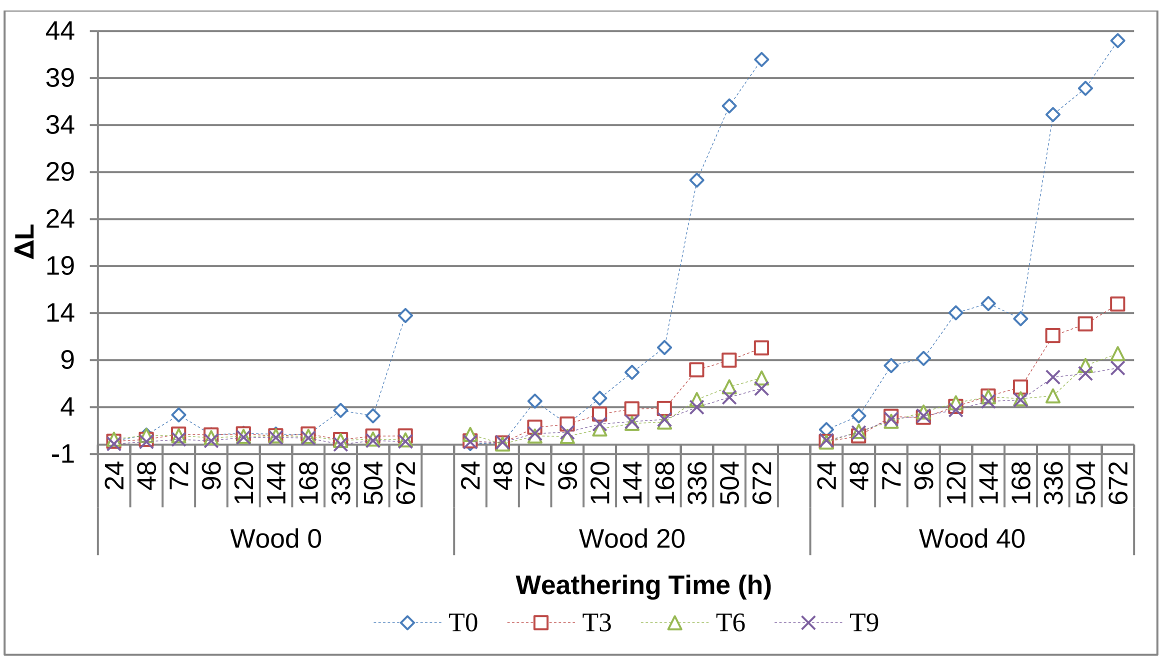

Fig. 15. The effects of weathering and fillers amount on Δ*L* values of WPCs

Examining the ΔL^* values graphs of the WPCs in Fig. 15, it can be seen that the ΔL^* value of neat PP increased, especially after the 336th hour, and the highest ΔL^* values for this group were determined as the measurement at the 672nd hour. Although the usage of TiO_2 in the composite groups that did not contain wood flour significantly increased the L^* values, the L^* values increased slightly with the enhancement in the amount of TiO_2. It has been observed that the ΔL^* values (at different weathering times) of the composite groups that do not contain wood flour but contain TiO_2 at different levels were in close ranges. The ΔL^* values of WPCs rose by the extension of weathering exposure time with the addition of wood flour into the matrix. Moreover, the effect of TiO_2 on ΔL^* values became more conspicuous with the loading of wood flour into the composites. With the addition of wood flour in all composite groups, the colors of the composites shifted from white to black on the color coordinates, while the colors of the composites shifted from black to white with the presence of TiO_2 in the WPCs. With the presence of white TiO_2 in WPCs, the lightness values were increased significantly. The lightness values increased significantly with the addition of the first 3% TiO_2 in the WPCs content, while slight increases were observed in the subsequent usage amounts. The UV stability of WPCs increased with the usage of TiO_2, and ΔL^* values decreased compared to the groups that did not use TiO_2. The ΔL^* values were determined in close ranges in WPC groups without wood flour content. With the weathering time, the ΔL^* values of WPCs containing TiO_2 slightly increased. It has been stated that TiO_2 nanoparticles decreased the UV intensity required for the oxidation of WPCs by absorbing UV radiation and thus playing an important role in delaying the photo-degradation process (Deka and Maji 2011). It has been reported that the UV stability of wood-flour-filled (Du *et al.* 2010) and montmorillonite clay-filled (Grigoriadou *et al.* 2011) HDPE-based composites increased with the usage of TiO_2. The weathering time and both fillers were significantly effective relative to the ΔL^* values of WPCs ($P < 0.0001$). In the sample groups that were not exposed to weathering, the lightness of samples in all composite groups decreased as the amount of wood flour increased. For the groups without TiO_2, the lightness of samples increased with the extension of the weathering time. In addition, the lightness of samples was also increased in these groups with rising wood flour content by prolonging the UV radiation exposure time. With degradation, cracks occurred on the polymer matrix surfaces, and wood fibers became prominent on the surface. Peng *et al.* (2014) stated that the increment of lightness with extended weathering time could be attributed to the protrusion of WF on the degraded surface. Lignin, one of the three basic components of wood, is more susceptible to UV light than cellulose and hemicellulose (Beg and Pickering 2008; Teacă *et al.* 2013). Some researchers attribute the discoloration of wood or lignocellulosic materials to the lignin and extractive substances in their content during exposure to intense weather conditions (Chen *et al.* 2016; Ouadou *et al.* 2017). With the degradation of lignin, cellulose, which is more stable against UV rays and has a white color, has become the main part of the deteriorated surface after degradation (Peng *et al.* 2014). Thus, the lightness values on the weathered surface increased.

When the total color changes (ΔE) of WPCs were examined, lesser ΔE values were obtained in the composite groups containing only TiO_2 than those that did not contain it. In these groups, slight increases were observed until the 168th hour with the increase in the exposure time to UV radiation, while slight improvements were observed in these values at the 336th hour and after. The ΔE values of the composite groups containing only wood flour showed an obvious increase with the increasing amount of wood flour and the weathering time compared to neat PP. While the Δ*E* values of the Neat PP group showed a significant change at the 336th hour and after, this change was observed in each period of weathering in the groups containing wood flour. From Fig. 16, there was a significant increase in the Δ*E* values of the composite groups containing wood flour, especially after the 168th hour, and measurements at the end of the 336th hour. It is thought that using TiO_2 in composite groups containing wood flour plays an important role in improving Δ*E* values. The effects of weathering time on Δ*E* values slightly decreased with the enhancement in the amount of TiO_2 usage in these WPC groups. This is thought to be due to the protective properties of TiO_2 against UV rays.

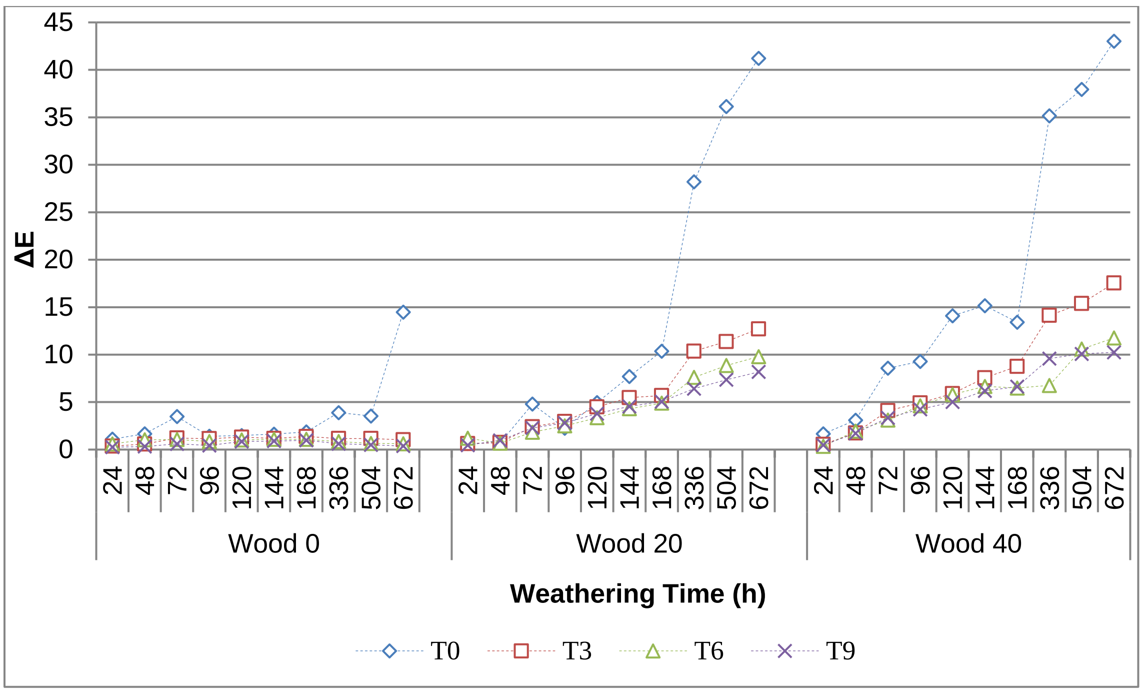

Fig. 16. The effects of weathering and fillers amount on Δ*E* values of WPCs

Effect of Weathering on Surface Roughness of WPCs

Results of the descriptive statistical analysis for the surface roughness of samples are summarized in Table 11. Surface roughness properties of samples classified by accelerated weathering cycles and sample compositions were reported according to the surface roughness parameter R_a. Intergroup variability is discussed in the inferential statistical analysis section. As shown in Table 11, considering the effects of weathering time on R_a values of WPCs and when all samples were collectively evaluated, the lowest R_a (5.845 µm) values were found in the unweathered samples, while the highest average roughness parameter values were observed as 8.881 µm in the samples exposed to 168 h of accelerated weathering. However, the highest R_a value was followed by the 8,760 µm, 8,629 µm, and 8,303 µm R_a values of the samples exposed to 672, 504, and 336 h of accelerated weathering, respectively. When Table 13, which presents Tukey multiple comparison results for accelerated aging cycles, is examined, it can be seen that there was no significant difference in the mean R_a values of the samples exposed to the effect of accelerated aging for 144, 168, 336, 504, 672 h. The lowest and highest range values for the R_a parameter were recorded at 4.659 µm for un-weathered samples (0 h) and at 13,832 μm for samples exposed to accelerated aging at the highest time (672 h). The lowest mean R_a roughness data (6.421 μm ± 1.358 μm) was recorded for the W0T0 group samples, and the highest mean R_a roughness data (8.674μm ± 3.072 μm) was recorded for the W40T0 group samples.

Table 11. Descriptive Statistical Data Classified by Accelerated Weathering Cycles and Sample Compositions

Surface Roughness Parameter	Weathering Time (h)	Number of Samples	Mean	Std. Dev.	Min.	Max.	Range
Ra	**0**	60	5.845	1.415	3.374	9.758	6.384
	24	60	7.612	2.135	4.319	13.251	8.932
	48	60	7.578	2.388	3.343	17.235	13.892
	72	60	7.370	1.790	4.093	11.663	7.570
	96	60	7.608	2.201	4.087	14.284	10.197
	120	60	7.237	2.055	3.708	14.965	11.257
	144	60	8.026	2.614	4.183	16.924	12.741
	168	60	8.881	1.971	5.503	12.988	7.485
	336	60	8.303	2.439	3.768	14.080	10.312
	504	60	8.629	2.540	4.124	16.657	12.533
	672	60	8.760	2.663	4.937	15.639	10.702
Ra	**W0T0**	55	6.421	1.358	4.126	9.912	5.786
	W0T3	55	6.830	2.246	3.768	13.415	9.647
	W0T6	55	8.626	2.525	4.517	17.235	12.718
	W0T9	55	7.434	2.076	4.124	13.251	9.127
	W20T0	55	8.655	3.172	4.087	16.657	12.570
	W20T3	55	8.248	1.956	4.493	12.943	8.450
	W20T6	55	7.074	1.632	4.183	10.435	6.252
	W20T9	55	8.289	2.210	4.576	14.080	9.504
	W40T0	55	8.674	3.072	4.225	15.639	11.414
	W40T3	55	8.558	2.524	4.845	16.924	12.079
	W40T6	55	6.995	1.970	3.343	11.663	8.320
	W40T9	55	7.847	1.410	4.507	10.775	6.268

The results of the two-way ANOVA analysis based on the stepwise regression principle performed at the 95% confidence interval of the weathered and un-weathered samples are presented in Table 12 for the dependent variable R_a.

Table 12. Two-Way ANOVA Analyses of R_a Surface Roughness

Source	DF	Adj SS	Adj MS	F-Value	P-Value
Composite content	11	404.1	36.733	15.77	< 0.0001
Weathering time	10	451.5	45.154	19.39	< 0.0001
Composite content * Weathering time	110	1595.9	14.508	6.23	< 0.0001
Error	528	1229.7	2.329		
Total	659	3681.2			

	R-sq	R-sq (adj)	R-sq (pred)
1.52608	66.60%	58.31%	47.81%

Table 12 shows that both the material composition group and the accelerated aging cycle independent variables were statistically significant factors in the 95% confidence interval. Furthermore, the interaction between composite content and weathering time was significant, with a p-value of < 0.0001. In contrast, it was determined that the model developed for the dependent variable R_a had an R^2 value of 66.60%.

When the main effects graph of the R_a parameter given in Fig. 17 is examined, more than 120 h of the accelerated aging cycles showed a more significant (roughness-enhancer) effect on the surface roughness of the samples compared to the first h. It was determined that the roughness data was partially horizontal in the cycles from the 24th hour to the 120th hour, and an increment in surface roughness occurred when proceeding from the 120th hour to the 672nd hour. Although this roughness increase cannot be associated with the gradually increasing TiO_2 amount, it can be seen from the graphs in Fig. 17 that increasing the wood content from 0% to 20% and then to 40% had an effect of increasing surface roughness.

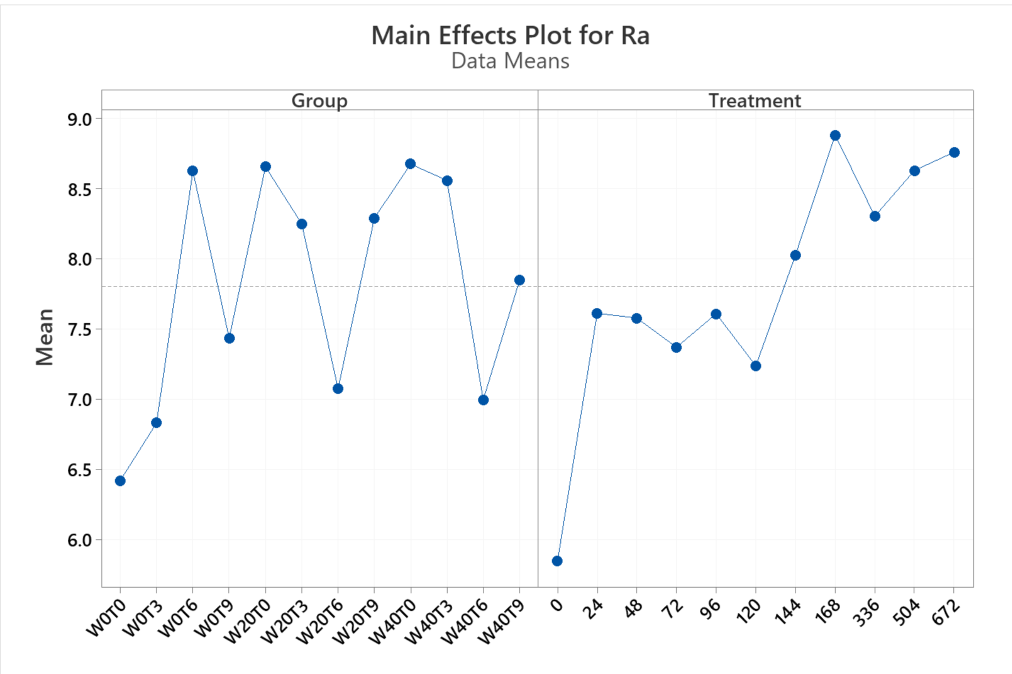

Fig. 17. The main effects graph for Ra variable

At the last stage of the inferential statistical analyses for surface roughness of samples, Tukey Multiple Comparison Results analyses were applied based on R_a roughness parameter values on groups with different material compositions exposed to periodically accelerated aging, and the results are reported in Tables 13 and 14. As a Tukey multiple comparison results, it was determined that the samples exposed to weathering for 168 h with un-weathered samples differed regarding R_a surface roughness. The mean surface roughness values measured after being exposed to accelerated weathering at five different higher times (144, 168, 336, 504, and 672 h) did not show a statistically significant difference. It was determined that the mean roughness values of the un-weathered samples and the mean roughness values of the samples exposed to accelerated weathering for a certain period of time had a statistically significant difference. These findings are in line with the results of other descriptive and inferential statistical analyses discussed above.

Table 13. Tukey Multiple Comparison Results for Accelerated Aging Cycles

Treatment	N	Mean	Grouping			
168	60	8.88133	A			
672	60	8.75980	A			
504	60	8.62867	A			
336	60	8.30330	A	B		
144	60	8.02573	A	B	C	
24	60	7.61217		B	C	
96	60	7.60823		B	C	
48	60	7.57760		B	C	
72	60	7.36989			C	
120	60	7.23748			C	
0	60	5.84513				D

Table 14. Tukey Multiple Comparison Results for Sample Compositions

Group	N	Mean	Grouping				
W40T0	55	8.67445	A				
W20T0	55	8.65495	A				
W0T6	55	8.62636	A				
W40T3	55	8.55818	A				
W20T9	55	8.28949	A	B			
W20T3	55	8.24846	A	B			
W40T9	55	7.84693	A	B	C		
W0T9	55	7.43444		B	C	D	
W20T6	55	7.07429			C	D	E
W40T6	55	6.99509			C	D	E
W0T3	55	6.83044				D	E
W0T0	55	6.42075					E

Means that do not share a letter are significantly different.

According to the results of Tukey multiple comparison results performed at the scale of groups with different material compositions, when all weathering cycles were collectively evaluated, it was observed that the most statistically differentiated groups in terms of R_a roughness findings were W0T6, which exhibited higher roughness characteristics, and W0T0 and W0T3 groups, which had lower roughness characteristics. It was observed that other groups exhibited similar roughness characteristics with at least one different group.

SEM images of sample surfaces were taken at 120 magnifications before and after weathering to determine the effects of accelerated weathering on the surface roughness of the samples (Fig. 18). When the SEM images before weathering are examined, it can be seen that the surfaces of the samples had similar structures in general. The particles in the yellow circle in Fig. 18-e and Fig. 18-g are thought to be small dust particles that adhere to the surface either during production or when taking SEM images. The particles in the yellow circle in Fig. 18-k are the wood fibers remaining on the surface. These images were obtained in some samples of the groups in which the lignocellulosic filler was used at the highest level. In these groups, the wood fibers, even if they were very small parts, were visualized on the surface, especially in images taken at high magnifications. The wood fibers appearing heavily on the composite surface are shown with yellow arrows In Fig. 18-l for the W40T9 group. With this image, it is possible to say that a large number of wood fibers appeared due to degradation on the polymer surfaces.

In the SEM images of the samples taken after weathering, the longitudinal and vertical cracks and their lengths are shown in yellow circles. After weathering, collapses occurred in some parts of the polymer matrices, while small voids were formed in some parts. With the usage of TiO_2 in the groups that did not contain wood flour, slightly better surface visuals were obtained compared to the groups that were not used. When the SEM images in Fig. 18-f through 18-j of WPCs groups containing wood flour are examined, it can be clearly seen that a rough surface was obtained after weathering. Furthermore, cracks occurred on the polymer matrix surfaces with degradation, and wood fibers became prominent on the surface.

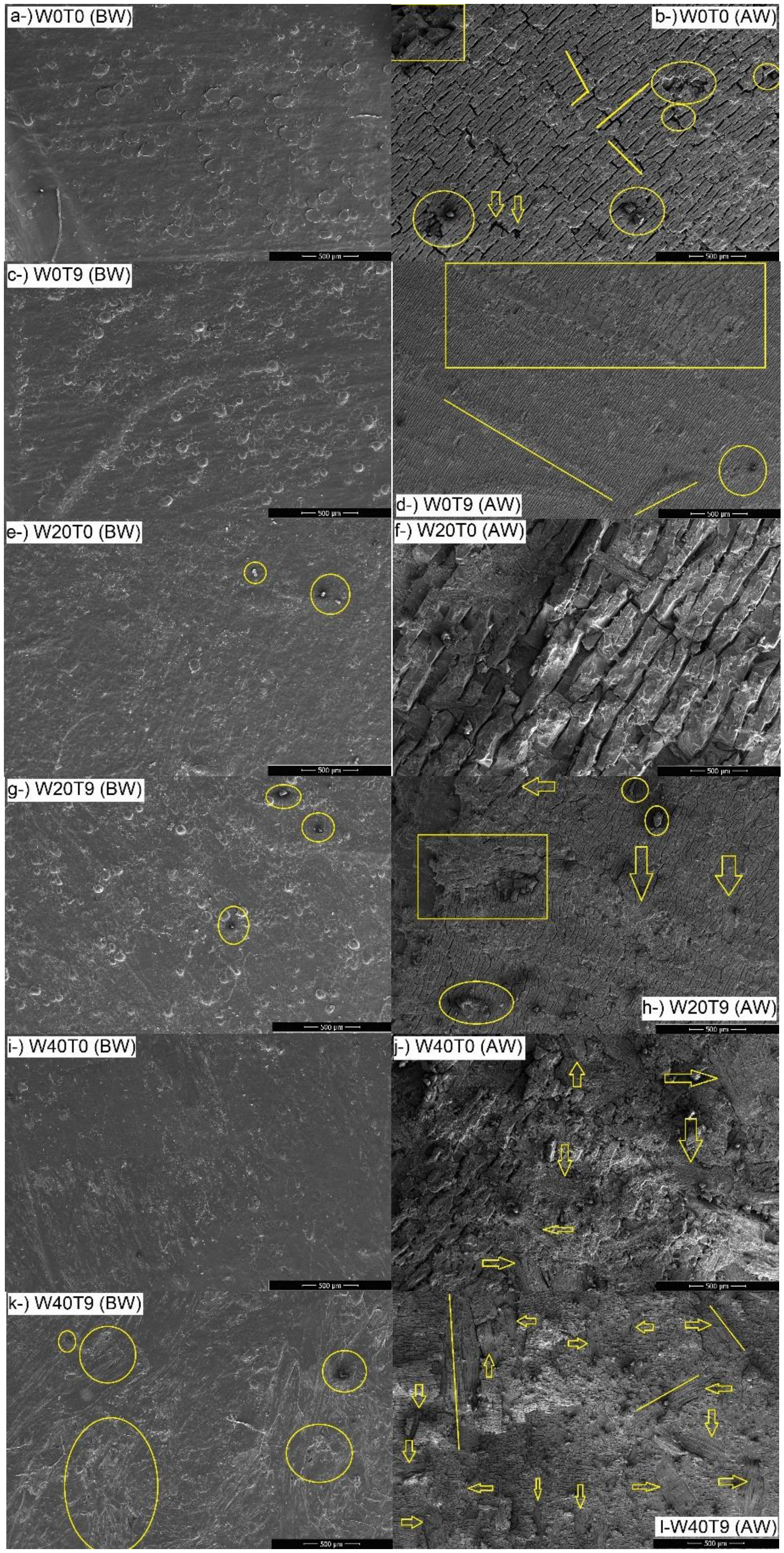

Fig. 18. SEM Images (taken at 200 magnification) of WPCs taken before (BW) and after (AW) weathering with a ETD Detector; a-) W0T0 (BW), b-) W0T0 (AW), c-) W0T9 (BW), d-) W0T9 (AW), e-) W20T0 (BW), f-) W20T0 (AW), g-) W20T9 (BW), h-) W20T9 (AW), i-) W40T0 (BW), j-) W40T0 (AW), k-) W40T9 (BW), and l-) W40T9 (AW)

The protrusions of wood flour on the degraded surface were visualized with these images. These images support the surface roughness findings. The agglomerations of nano TiO_2 in the WPCs' decomposition surface were visualized with SEM images, taken at 5000 magnification, with the help of a CBS detector after weathering. The SEM images of the W40T6 and the W40T9 groups are presented in Figs. 19-a and 19-b, respectively. From these SEM images, it was observed that aggregations formed with the usage of nano TiO_2 at high levels, and these agglomerations increased with increased TiO_2 amount. In addition, these images helped to explain the fluctuations in the mechanical strength values of the groups in which TiO_2 was used at high levels.

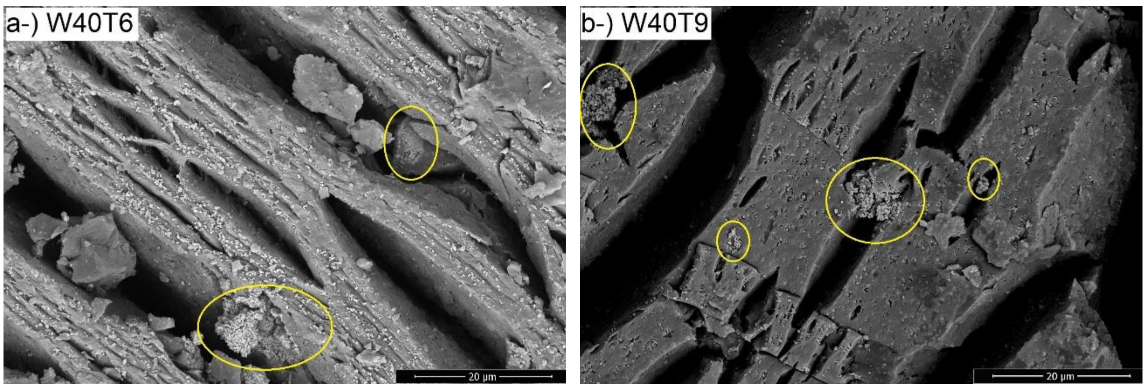

Fig. 19. SEM Images (taken at 5000 magnification) of WPCs with a CBS Detector; a-) W40T6, b-) W40T9

CONCLUSIONS

This study evaluated the effect of Iroko wood flours and nano-TiO_2 concentration on the accelerated weathering resistance and tribological, thermal, physical, mechanical, and morphological properties of wood fiber (WF) and TiO_2-reinforced polypropylene (PP)-based composites. Physical (density and hardness), thermal (TGA and DSC), tribological (friction coefficient (CoF) and the specific wear rate (WR)), mechanical (tensile, flexural, and impact strength), and morphological properties (SEM) properties were determined. In addition, mechanical, color changes (total color changes and color changes in lightness), surface roughness, and morphological properties of wood polymer composite (WPC) samples were determined after exposure to accelerated weathering. As a result, the following conclusions were reached:

1. PP-based composites with acceptable properties were manufactured utilizing varying concentrations of Iroko wood flour (WF) and nano-titanium dioxide (TiO_2) as fillers.
2. The WF and nano-TiO_2 significantly affect the density and hardness values of the composites. Increases in density and hardness values are observed with the presence of both fillers in the polymer matrix.
3. In WPC groups containing the maximum wood flour amount (40%), the mechanical properties were affected at high usage amounts of TiO_2 due to agglomeration of the nanomaterial.

4. The presence of TiO_2, which has higher thermal stability than wood flour, in WPCs, also increased their thermal stability, and the amount of residues at 600 °C increased with the usage of both fillers. Both fillers tended to decrease the crystallinity of the polymer, but wood flour loading reduced the crystallinity of the composites to a greater extent than TiO_2 loading.
5. The coefficient of friction properties was improved with the usage of both fillers. Moreover, a synergetic effect occurred on the WR properties of WPCs with the usage of both fillers together.
6. The presence of both fillers in the polymer matrix had positive effects on the tensile strength (TS), flexural strength (FS), and flexural modulus (MOE) of the composites. In contrast, EatB values decreased with the usage of both fillers. The presence of wood flour in the matrix positively affected impact strength (IS) values, while TiO_2 had a negative affect.
7. Weathering time had a significant effect on the mechanical strength values of WPCs. The group that showed the most change in the mechanical properties with the prolongation of weathering exposure time was the neat-PP group. Both fillers demonstrated a protective effect against UV radiation and resulted in either slight increases in the mechanical strength of WPCs containing the fillers or minimized the negative effects following weathering. These findings highlight the beneficial impact of fillers in enhancing the resistance of WPCs to weathering conditions.
8. The incorporation of wood flour and TiO_2 demonstrated a noteworthy influence on the total color changes (ΔE) and color changes in lightness (ΔL^*) properties. Specifically, the utilization and increased usage amount of wood flour exhibited a predominantly negative impact on these properties. Conversely, TiO_2 exhibited a protective effect against UV radiation, thereby mitigating the negative effects on the aforementioned color properties. These findings underscore the significance of wood flour and TiO_2 as influential factors in the alteration of color characteristics in response to UV exposure.
9. The surface roughness characteristics of the WPCs were significantly influenced by both the duration of weathering and the amount of wood flour incorporated. Particularly, the surface roughness of the WPCs exhibited a notable increase, particularly when exposed to weathering for 168 h or longer, as well as with higher levels of wood flour content. These observations emphasize the pronounced impact of weathering time and wood flour content on the surface roughness properties of the WPCs.

ACKNOWLEDGEMENT

This research was supported by Kütahya Dumlupınar University, Research Project Coordination Unit, under project number: 2022-38.

REFERENCES CITED

Ahalwan, A., and Yousif, B. F. (2013). "In state of art: Mechanical and tribological behaviour of polymeric composites based on natural fibres," *Materials and Design* (48), 14-24. DOI: 10.1016/j.matdes.2012.07.014

Al-Maqdasi, Z., Jantel, U., Joffe, R., and Emami, N. (2022). "Tribological study on wood and graphene reinforced high density polyethylene," in: *Composites Meet Sustainability -Proceedings of the 20th European Conference on Composite Materials (ECCM20),* Lausanne, Switzerland, pp. 1-8. (26-30 June, 2022)

Alsan, M. (2016). *Isıl İşlem Görmüş Odunun Polipropilen Kompozitlerin Özellikleri Üzerine Etkileri [The Effects of Heat-treated Wood on the Propertıes of Polypropylene Composıtes],* Master's Thesis, Bartın University, Bartın, Türkiye.

Annie Paul, S., Boudenne, A., Ibos, L., Candau, Y., Joseph, K., and Thomas, S. (2008). "Effect of fiber loading and chemical treatments on thermophysical properties of banana fiber/polypropylene commingled composite materials," *Composites Part A: Applied Science and Manufacturing* 39(9), 1582-1588. DOI: 10.1016/j.compositesa.2008.06.004

Ashori, A., and Nourbakhsh, A. (2011). "Preparation and characterization of polypropylene/wood flour/nanoclay composites," *European Journal of Wood and Wood Products* 69(4), 663-666. DOI: 10.1007/s00107-010-0488-9

ASTM D256 (2010). "Standard test for determining the izod pendulum impact resistance of plastics," ASTM International, West Conshohocken, PA, USA.

ASTM D638 (2010). "Standard test for tensile properties of plastics," ASTM International, West Conshohocken, PA, USA.

ASTM D2240 (2017). "Standard test method for rubber property-durometer hardness," ASTM International, West Conshohocken, PA, USA.

ASTM D2244 (2009). "Standard pratice for calculation of color tolerances and color differences from instrumentally measured color coordinates," ASTM International, West Conshohocken, PA, USA.

ASTM D790 (2010). "Standard test methods for flexural properties of unreinforced and reinforced plastics and electrical insulating materials," ASTM International, West Conshohocken, PA, USA.

ASTM D792 (2008). "Standard test methods for density and specific gravity (relative density) of plastics by displacement," ASTM International, West Conshohocken, PA, USA.

ASTM D6662 (2001). "Standard specification for polyolefin-based plastic lumber decking boards," ASTM International, West Conshohocken, PA, USA.

ASTM G154 (2011). "Standard practice for operating fluorescent ultraviolet (UV) lamp apparatus for exposure of nonmetallic materials," ASTM International, West Conshohocken, PA, USA.

ASTM G99-17 (2017). "Standard test method for wear testing with a pin-on-disk apparatus," ASTM International, West Conshohocken. DOI: 10.1520/G0099-17.Copyright

Aurrekoetxea, J., Sarrionandia, M., and Gomez, X. (2008). "Effects of microstructure on wear behaviour of wood reinforced polypropylene composite," *Wear* 265(5-6), 606-611. DOI: 10.1016/j.wear.2007.12.013

Aydemir, D., Alsan, M., Can, A., Altuntas, E., and Sivrikaya, H. (2019). "Accelerated weathering and decay resistance of heat-treated wood reinforced polypropylene composites," *Drvna Industrija* 70(3), 279-285. DOI: 10.5552/drvind.2019.1851

Aydemir, D., Uzun, G., Gumuş, H., Yildiz, S., Gumuş, S., Bardak, T., and Gunduz, G. (2016). "Nanocomposites of polypropylene/nano titanium dioxide: Effect of loading rates of nano titanium dioxide," *Medziagotyra* 22(3), 364-369. DOI: 10.5755/j01.ms.22.3.8217

Badji, C., Soccalingame, L., Garay, H., Bergeret, A., and Bénézet, J. C. (2017). "Influence of weathering on visual and surface aspect of wood plastic composites: Correlation approach with mechanical properties and microstructure," *Polymer Degradation and Stability* 137, 162-172. DOI: 10.1016/j.polymdegradstab.2017.01.010

Bajpai, P. K., Singh, I., and Madaan, J. (2012). "Frictional and adhesive wear performance of natural fibre reinforced polypropylene composites," *Proceedings of the Institution of Mechanical Engineers, Part J: Journal of Engineering Tribology* 227(4), 385-392. DOI: 10.1177/1350650112461868

Basalp, D., Tihminlioglu, F., Sofuoglu, S. C., Inal, F., and Sofuoglu, A. (2020). "Utilization of municipal plastic and wood waste in industrial manufacturing of wood plastic composites," *Waste and Biomass Valorization* 11(10), 5419-5430. DOI: 10.1007/s12649-020-00986-7

Başboğa, İ. H., Atar, İ., Karakuş, K., and Mengeloğlu, F. (2020). "Determination of some technological properties of injection molded pulverized-HDPE based composites reinforced with micronized waste tire powder and red pine wood wastes," *Journal of Polymers and the Environment* 28(6), 1776-1794. DOI: 10.1007/s10924-020-01726-7

Başboğa, İ. H., Kılıç, İ., Ata, İ., and Mengeloğlu, F. (2022). "Tropik ağaç türü olan dahoma (*Piptadeniastrum africanum*) odununun odun plastik kompozit üretiminde kullanımı [The usage of wood of dahoma (*Piptadeniastrum Africanum*), a tropic tree, in the production of wood plastic composite]," *Ormancılık Araştırma Dergisi [Forestry Research Journal]* 9(Özel Sayı [Special Issue]), 271-280. DOI: 10.17568/ogmoad.1091247

Bazan, P., Salasińska, K., and Kuciel, S. (2021). "Flame retardant polypropylene reinforced with natural additives," *Industrial Crops and Products* 164, article ID 113356. DOI: 10.1016/j.indcrop.2021.113356

Behravesh, A. H., Shakouri, E., Zolfaghari, A., and Golzar, M. (2010). "Theoretical and experimental study on die pressure prediction in extrusion of wood-plastic composite," *Journal of Composite Materials* 44(11), 1293-1304. DOI: 10.1177/0021998309352703

Beg, M. D. H., and Pickering, K. L. (2008). "Accelerated weathering of unbleached and bleached kraft wood fibre reinforced polypropylene composites," *Polymer Degradation and Stability* 93(10), 1939-1946. DOI: 10.1016/j.polymdegradstab.2008.06.012

Birleanu, C., Pustan, M., Cioaza, M., Molea, A., Popa, F., and Contiu, G. (2022). "Effect of TiO_2 nanoparticles on the tribological properties of lubricating oil: An experimental investigation," *Scientific Reports* 12(1), article 5201. DOI: 10.1038/s41598-022-09245-2

Boran Torun, S., Tomak, E. D., Donmez Cavdar, A., and Mengeloglu, F. (2021). "Characterization of weathered MCC / nutshell reinforced composites," *Polymer Testing* 101, article ID 107290. DOI: 10.1016/j.polymertesting.2021.107290

Brostow, W., Datashvili, T., Jiang, P., and Miller, H. (2016). "Recycled HDPE reinforced with sol-gel silica modified wood sawdust," *European Polymer Journal* 76, 28-39. DOI: 10.1016/j.eurpolymj.2016.01.015

Burgada, F., Fages, E., Quiles-Carrillo, L., Lascano, D., Ivorra-Martinez, J., Arrieta, M. P., and Fenollar, O. (2021). "Upgrading recycled polypropylene from textile wastes in wood plastic composites with short hemp fiber," *Polymers* 13(8), article 1248. DOI: 10.3390/polym13081248

Carus, M., and Eder, A. (2015). *Biocomposites: 352,000 t of Wood and Natural Fibre Composites Produced in the European Union in 2012 – Executive Summary* (Version 2015-05), Nova-Institut GmbH, Hürth, Germany.

Çavuş, V. (2017). *Farkli Erime Akiş Indeksine Sahip Polipropilen Esasli Ahşap Polimer Kompozitlerin Özelliklerinin Belirlenmesi [Determining the Properties of the Polypropylene Based Wood-Polymer Composites with Different Melt Flow Index]*, Ph.D, Dissertation, Kahramanmaraş Sütçü İmam University, Kahramanmaraş, Türkiye.

Çavuş, V. (2020). "Selected properties of mahogany wood flour filled polypropylene composites: The effect of maleic anhydride-grafted polypropylene (MAPP)," *BioResources* 15(2), 2227-2236. DOI: 10.15376/biores.15.2.2227-2236

Çavuş, V., and Mengeloğlu, F. (2016). "Utilization of synthetic based mineral filler in wood plastics composite," *Journal of Achievements in Materials and Manufacturing Engineering* 77(2), 57-63.

Çavuş, V., and Mengeloğlu, F. (2020). "Effect of wood particle size on selected properties of neat and recycled wood polypropylene composites," *BioResources* 15(2), 3427-3442. DOI: 10.15376/biores.15.2.3427-3442

Chen, W. H., Eng, C. F., Lin, Y. Y., and Bach, Q. V. (2020). "Independent parallel pyrolysis kinetics of cellulose, hemicelluloses and lignin at various heating rates analyzed by evolutionary computation," *Energy Conversion and Management* 221, article ID 113165. DOI: 10.1016/j.enconman.2020.113165

Chen, Y., Stark, N. M., Tshabalala, M. A., Gao, J., and Fan, Y. (2016). "Weathering characteristics of wood plastic composites reinforced with extracted or delignifiedwood flour," *Materials* 9(8), article 610. DOI: 10.3390/ma9080610

Clemons, C. M. (2002). "Wood-plastic composites in the United States: The interfacing of two industries," *Forest Products Journal* 52(6), 10-18.

Deka, B. K., and Maji, T. K. (2011). "Effect of TiO_2 and nanoclay on the properties of wood polymer nanocomposite," *Composites Part A: Applied Science and Manufacturing* 42(12), 2117-2125. DOI: 10.1016/j.compositesa.2011.09.023

Dönmez Çavdar, A., Tomak, E. D., Boran Torun, S., and Arpaci, S. S. (2021). "Accelerated weathering resistance of high-density polyethylene composites reinforced with microcrystalline cellulose and fire retardants," *Journal of Building Engineering* 39, article ID 102282. DOI: 10.1016/j.jobe.2021.102282

Du, H., Wang, W., Wang, Q., Zhang, Z., Sui, S., and Zhang, Y. (2010). "Effects of pigments on the UV degradation of wood-flour/HDPE composites," *Journal of Applied Polymer Science* 118, 1068-1076. DOI: 10.1002/app.32430

Dwivedi, U. K., and Chand, N. (2008). "Influence of wood flour loading on tribological behavior of epoxy composites," *Polymer Composites,* article ID 15480569. DOI: 10.1002/pc.20548

Ekşioğlu. (2022). *Türkiye'de Yoğun Talep Gören Afrika Ağaçları [The High Demand*

African Trees in Turkey], The Product Catalog of Ekşioğlu Forest Products Company, Kocaeli, Türkiye.

EN 338:2009 (2009). "Structural timber—Strength classes," European Committee for Standardization, Brussels, Belgium.

Erem, A. D., Ozcan, G., and Skrifvars, M. (2013). "*In vitro* assessment of antimicrobial polypropylene/zinc oxide nanocomposite fibers," *Textile Research Journal* 83(20), 2152-2163. DOI: 10.1177/0040517513490060

Esmizadeh, E., Tzoganakis, C., and Mekonnen, T. H. (2020). "Degradation behavior of polypropylene during reprocessing and its biocomposites: Thermal and oxidative degradation kinetics," *Polymers* 12(8), article 1627. DOI: 10.3390/polym12081627

Fabiyi, J. S., and McDonald, A. G. (2014). "Degradation of polypropylene in naturally and artificially weathered plastic matrix composites," *Maderas: Ciencia y Tecnologia* 16(3), 275-290. DOI: 10.4067/S0718-221X2014005000021

Foong, S. Y., Liew, R. K., Yang, Y., Cheng, Y. W., Yek, P. N. Y., Wan Mahari, W. A., Lee, X. Y., Han, C. S., Vo, D. V. N., Van Le, Q., *et al.* (2020). "Valorization of biomass waste to engineered activated biochar by microwave pyrolysis: Progress, challenges, and future directions," *Chemical Engineering Journal* 389, article ID 124401. DOI: 10.1016/j.cej.2020.124401

Geert, R., and Kuilen, J. W. (2010). "Comparison of methods of strength classification of tropical hardwood timber," in: *The Eleventh World Conference on Timber Engineering*, Riva Del Garda, Italy.

Ghalehno, M. D., Kord, B., and Sheshkal, B. N. (2020). "Mechanical and physical properties of wood/polyethylene composite reinforced with TiO_2 nanoparticles," *Cerne* 26(4), 474-481. DOI: 10.1590/01047760202026042753

Grigoriadou, I., Paraskevopoulos, K. M., Chrissafis, K., Pavlidou, E., Stamkopoulos, T. G., and Bikiaris, D. (2011). "Effect of different nanoparticles on HDPE UV stability," *Polymer Degradation and Stability* 96(1), 151-163. DOI: 10.1016/j.polymdegradstab.2010.10.001

Hamdan, S., Mun'aim, M. A., Idrus, M., Rahman, R., Ibrahim, N. F., and Islam, M. S. (2010). "Wear of wood polymer composite for journal bearing materials," *Wood Research Journal* 1(1), 22-26.

Han, G., Lei, Y., Wu, Q., Kojima, Y., and Suzuki, S. (2008). "Bamboo-fiber filled high density polyethylene composites: Effect of coupling treatment and nanoclay," *Journal of Polymers and the Environment* 16(2), 123-130. DOI: 10.1007/s10924-008-0094-7

Hazarika, A., and Maji, T. K. (2013). "Synergistic effect of nano-TiO_2 and nanoclay on the ultraviolet degradation and physical properties of wood polymer nanocomposites," *Industrial and Engineering Chemistry Research* 52(38), 13536-13546. DOI: 10.1021/ie401596h

Hou, X., Hu, Y., Hu, X., and Jiang, D. (2018). "Poly (ether ether ketone) composites reinforced by graphene oxide and silicon dioxide nanoparticles: Mechanical properties and sliding wear behavior," *High Performance Polymers* 30(4), 406-417. DOI: 10.1177/0954008317701549

Hung, K. C., Chen, Y. L., and Wu, J. H. (2012). "Natural weathering properties of acetylated bamboo plastic composites," *Polymer Degradation and Stability* 97(9), 1680-1685. DOI: 10.1016/j.polymdegradstab.2012.06.016

Ibrahim, M. A., Hirayama, T., and Khalafallah, D. (2019). "An investigation into the tribological properties of wood flour reinforced polypropylene composites," *Materials Research Express* 7(1), article ID 015313. DOI: 10.1088/2053-1591/ab600c

Ismail, H., Edyham, M. R., and Wirjosentono, B. (2002). "Bamboo fibre filled natural rubber composites: The effects of filler loading and bonding agent," *Polymer Testing* 21(2), 139-144. DOI: 10.1016/S0142-9418(01)00060-5

ISO-21920-2 (2021). "Geometrical product specifications (GPS) — Surface texture: Profile — Part 2: Terms, definitions and surface texture parameters," International Organization for Standardization, Geneva, Switzerland.

Jiang, L., He, C., Fu, J., and Chen, D. (2017). "Wear behavior of wood-plastic composites in alternate simulated sea water and acid rain corrosion conditions," *Polymer Testing* 63, 236-243. DOI: 10.1016/j.polymertesting.2017.08.031

Jiang, L., He, C., Li, X., and Fu, J. (2018). "Wear properties of wood-plastic composites pretreated with a stearic acid-palmitic acid mixture before exposure to degradative water conditions," *BioResources* 13(2), 3817-3831.

Johnson, B. (2020). "Wood plastic composite (WPC) market production values and generate revenue of USD 9953.8 million with a CAGR of 9.5% worldwide by 2030," (http://www.apnews.com) Accessed 07 Feb 2022.

Karmarkar, A., Chauhan, S. S., Modak, J. M., and Chanda, M. (2007). "Mechanical properties of wood–fiber reinforced polypropylene composites: Effect of a novel compatibilizer with isocyanate functional group," *Composites Part A: Applied Science and Manufacturing* 38(2), 227-233. DOI: 10.1016/J.COMPOSITESA.2006.05.005

Kaymakci, A. (2019). "Effect of titanium dioxide on some mechanical, thermal, and surface properties of wood-plastic nanocomposites," *BioResources* 14(1), 1969-1979. DOI: 10.15376/biores.14.1.1969-1979

Klyosov, A. (2007). *Wood Plastic Composite,* Wiley Interscience Publication, Hoboken, NJ, USA.

Kord, B., Hemmasi, A. H., and Ghasemi, I. (2011). "Properties of PP/wood flour/organomodified montmorillonite nanocomposites," *Wood Science and Technology* 45(1), 111-119. DOI: 10.1007/s00226-010-0309-7

Latha, P. S., Rao, M. V., Kumar, V. V. K., Raghavendra, G., Ojha, S., and Inala, R. (2016). "Evaluation of mechanical and tribological properties of bamboo–glass hybrid fiber reinforced polymer composite," *Journal of Industrial Textiles* 46(1), 3-18. DOI: 10.1177/1528083715569376

Lee, C. H., Hung, K. C., Chen, Y. L., Wu, T. L., Chien, Y. C., and Wu, J. H. (2012). "Effects of polymeric matrix on accelerated UV weathering properties of wood-plastic composites," *Holzforschung* 66(8), 981-987. DOI: 10.1515/hf-2011-0198

Li, K., Xiang, D., and Lei X. (2008). "Green and self-lubrication polyoxymethylene composites filled with low-density polyethylene and rice husk flour," *Journal of Applied Polymer Science* 108, 2778-2786. DOI: 10.1002/app.27603

Lu, N., and Oza, S. (2013). "A comparative study of the mechanical properties of hemp fiber with virgin and recycled high density polyethylene matrix," *Composites Part B: Engineering* 45(1), 1651-1656. DOI: 10.1016/j.compositesb.2012.09.076

Matuana, L. M., Park, C. B., and Balatinecz, J. J. (1998). "Cell morphology and property relationships of microcellular foamed PVC / wood-fiber composites," *Polymer Engineering and Science* 38(11), 1862-1872.

Mazzanti, V., Mollica, F., and El Kissi, N. (2016). "Rheological and mechanical characterization of polypropylene-based wood plastic composites," *Polymer Composites* 37(12), 3460-3473.

Mazzanti, V., Fortini, A., Malagutti, L., Ronconi, G., and Mollica, F. (2021). "Tribological behavior of a rubber-toughened wood polymer composite," *Polymers* 13, article ID 2055. DOI: 10.3390/polym13132055

Mengeloğlu, F., and Çavuş, V. (2021). "Long term natural weathering of PP based WPCs: The effect of TiO_2 on selected color, physical, mechanical, morphological and chemical properties," in: *Wood Polymer Composites*, S. M. Rangappa, J. Parameswaranpillai, M. H. Kumar, and S. Siengchin (eds.), Springer Singapore, Singapore, pp. 213-232.

Mengeloglu, F., and Kabakci, A. (2008). "Determination of thermal properties and morphology of eucalyptus wood residue filled high density polyethylene composites," *International Journal of Molecular Sciences* 9(2), 107-119. DOI: 10.3390/ijms9020107

Mengeloğlu, F., and Karakuş, K. (2008). "Some properties of eucalyptus wood flour filled recycled high density polyethylene polymer-composites," *Turkish Journal of Agriculture and Forestry* 32(6), 537-546. DOI: 10.3906/tar-0801-7

Mengeloglu, F., and Karakus, K. (2008). "Thermal degradation, mechanical properties and morphology of wheat straw flour filled recycled thermoplastic composites," *Sensors* 8(1), 500-519. DOI: 10.3390/s8010500

Mengeloğlu, F., Başboğa, İ., and Aslan, T. (2015). "Selected properties of furniture plant waste filled thermoplastic composites," *Proligno* 11(4), 199-206.

Mengeloglu, F., Kurt, R., Gardner, D. J., and O'Neill, S. (2007). "Mechanical properties of extruded high density polyethylene and polypropylene wood flour decking boards," *Iranian Polymer Journal* 16(7), 477-487.

Mrówka, M., Szymiczek, M., and Skonieczna, M. (2021). "The impact of wood waste on the properties of silicone-based composites," *Polymers* 13(7), article 7. DOI: 10.3390/polym13010007

Mylsamy, B., Chinnasamy, V., Palaniappan, S. K., Subramani, S. P., and Gopalsamy, C. (2020). "Effect of surface treatment on the tribological properties of *Coccinia indica* cellulosic fiber reinforced polymer composites," *Journal of Materials Research and Technology* 9(6), 16423-16434. DOI: 10.1016/j.jmrt.2020.11.100

Mysiukiewicz, O., and Sterzyński, T. (2017). "Influence of water on tribological properties of wood-polymer composites," *Arch. Mech. Tech. Mater.*Vol. 37, 79-84. DOI: 10.1515/amtm-2017-0013

Nirmal, U., Yousif, B. F., Rilling, D., and Brevern, P. V. (2010). "Effect of betelnut fibres treatment and contact conditions on adhesive wear and frictional performance of polyester composites," *Wear* 268(11-12), 1354-1370. DOI: 10.1016/j.wear.2010.02.004

Nourbakhsh, A., and Ashori, A. (2008). "Highly fiber-loaded composites: Physical and mechanical properties," *Polymers and Polymer Composites* 16(5), 343-347. DOI: 10.1177/096739110801600508

Ouadou, Y., Aliouche, D., Thevenon, M. F., and Djillali, M. (2017). "Characterization and photodegradation mechanism of three Algerian wood species," *Journal of Wood Science* 63(3), 288-294. DOI: 10.1007/s10086-017-1615-6

Ouinsavi, C., Sokpon, N., and Bada, O. (2005). "Utilization and traditional strategies of *in situ* conservation of iroko (*Milicia excelsa* Welw. C.C. Berg) in Benin," *Forest*

Ecology and Management 207(3), 341-350. DOI: 10.1016/j.foreco.2004.10.069
Özbey, F. (2018). *Hidrotermal Metot Ile TiO_2 Esasli Kompozit Malzemelerin Üretilmesi [Fabrication of Cadmium (Cd) Doped Titanium Dioxide (TiO_2) Based Composite Thin Film Materials]*, Master's Thesis, Fırat University, Elazığ, Türkiye.
Özdemir, F., Serin, Z. O., and Mengeloğlu, F. (2013). "Utilization of red pepper fruit stem as reinforcing filler in plastic composites," *BioResources* 8(4), 5299-5308. DOI: 10.15376/biores.8.4.5299-5308
Pang, A. L., and Ismail, H. (2014). "Influence of kenaf form and loading on the properties of kenaf-filled polypropylene/waste tire dust composites: A comparison study," *Journal of Applied Polymer Science* 131(19), 2-7. DOI: 10.1002/app.40877
Peng, Y., Liu, R., and Cao, J. (2014). "Effects of antioxidants on photodegradation of wood flour/polypropylene composites during artificial weathering," *BioResources* 9(4), 5817-5830. DOI: 10.15376/biores.9.4.5817-5830
Petkim (2016). *Petoplen EH102 Polipropilen (PP)*, Data sheet, Petkim Ltd., Co., İzmir, Türkiye.
Rahman, M. R., Hamdan, S., and Chang Hui, J. L. (2017). "Differential scanning calorimetry (DSC) and thermogravimetric analysis (TGA) of wood polymer nanocomposites," in: *MATEC Web of Conferences* 87, article 03013. DOI: 10.1051/matecconf/20178703013
Ramezani Kakroodi, A., Kazemi, Y., and Rodrigue, D. (2013). "Mechanical, rheological, morphological and water absorption properties of maleated polyethylene/hemp composites: Effect of ground tire rubber addition," *Composites Part B: Engineering* 51, 337-344. DOI: 10.1016/j.compositesb.2013.03.032
Ranakoti, L., Gupta, M. K., and Rakesh, P. K. (2019). "Analysis of mechanical and tribological behavior of wood flour filled glass fiber reinforced epoxy composite," *Mater. Res. Express* 6(8), article ID 085327. DOI: 10.1007/s12649-020-00986-7
Rao, J., Zhou, Y., and Fan, M. (2018). "Revealing the interface structure and bonding mechanism of coupling agent treated WPC," *Polymers* 10(3), article 266. DOI: 10.3390/polym10030266
Rashed, A., and Nabhan, A. (2018). "Effects of TiO_2 and SiO_2 nano additive to engine lubricant oils on tribological properties at different temperatures," in: *Proceedings of the 4th International Conference on Mechanical, Automotive And Aerospace Engineering (ICMAAE'18)*, Rome, Italy, pp. 2463-2472.
Richard, S., Rajadurai, J. S., and Manikandan, V. (2017). "Effects of particle loading and particle size on tribological properties of biochar particulate reinforced polymer composites," *Journal of Tribology* 139(1), article ID 012202. DOI: 10.1115/1.4033131
Rivera-Armenta, J. L., Salazar-Cruz, B. A., Espindola-Flores, A. C., Villarreal-Lucio, D. S., De León-Almazán, C. M., and Estrada-Martinez, J. (2022). "Thermal and thermomechanical characterization of polypropylene-seed shell particles composites," *Applied Sciences* 12(16), article 8336. DOI: 10.3390/app12168336
Rong, M. Z., Zhang, M. Q., and Ruan, W. H. (2006). "Surface modification of nanoscale fillers for improving properties of polymer nanocomposites: A review," *Materials Science and Technology* 22(7), 787-796. DOI: 10.1179/174328406X101247
Saeed, K., Park, S.-Y., and Ali, N. (2009). "Characterization of poly(butylene terephthalate) electrspun nanofibres containing titanium oxide," *Iranian Polymer Journal* 18(8), 671-677.

Saeed, U., Nawaz, M. A., and Al-Turaif, H. A. (2018). "Wood flour reinforced biodegradable PBS/PLA composites," *Journal of Composite Materials* 52(19), 2641-2650. DOI: 10.1177/0021998317752227

Sain, M., and Panthapulakkal, S. (2006). "Bioprocess preparation of wheat straw fibers and their characterization," *Industrial Crops and Products* 23(1), 1-8. DOI: 10.1016/j.indcrop.2005.01.006

Samyn, P., and Schoukens, G. (2009). "Thermochemical sliding interactions of short carbon fiber polyimide composites at high pv-conditions," *Materials Chemistry and Physics* 115(1), 185-195. DOI: 10.1016/j.matchemphys.2008.11.029

Santiagoo, R., Ismail, H., and Hussin, K. (2011). "Mechanical properties, water absorption, and swelling behaviour of rice husk powder filled polypropylene/recycled acrylonitrile butadiene rubber (pp/nbrr/rhp) biocomposites using silane as a coupling agent," *BioResources* 6(4), 3714-3726. DOI: 10.15376/biores.6.4.3714-3726

Stark, N. M. (2007). "Considerations in the weathering of wood-plastic composites," in: *3rd Wood Fibre Polymer Composites International Symposium*, Bordeaux, France.

Stark, N. M., and Matuana, L. M. (2007). "Characterization of weathered wood-plastic composite surfaces using FTIR spectroscopy, contact angle, and XPS," *Polymer Degradation and Stability* 92(10), 1883-1890. DOI: 10.1016/j.polymdegradstab.2007.06.017

Steckel, V., Clemons, C. M., and Thoemen, H. (2007). "Effects of material parameters on the diffusion and sorption properties of wood-flour/polypropylene composites," *Journal of Applied Polymer Science* 113, 752-763. DOI: 10.1002/app.25037

Suryawanshi, S. R., and Pattiwar, J. T. (2018). "Effect of TiO_2 nanoparticles blended with lubricating oil on the tribological performance of the journal bearing," *Tribology in Industry* 40(3), 370-391. DOI: 10.24874/ti.2018.40.03.04

Tai, Z., Chen, Y., An, Y., Yan, X., and Xue, Q. (2012). "Tribological behavior of UHMWPE reinforced with graphene oxide nanosheets," *Tribology Letters* 46(1), 55-63. DOI: 10.1007/s11249-012-9919-6

Tasdemir, C., Basboga, I. H., and Hiziroglu, S. (2020). "Surface quality of wood plastic composites as function of water exposure," *Applied Sciences* 10(15), aritcle 5122. DOI: 10.3390/app10155122

Teacă, C. A., Roşu, D., Bodîrlău, R., and Roşu, L. (2013). "Structural changes in wood under artificial UV light irradiation determined by FTIR spectroscopy and color measurements – A brief review," *BioResources* 8(1), 1478-1507. DOI: 10.15376/biores.8.1.1478-1507

Várhegyi, G., Szabó, P., and Antal, M. J. (1994). "Kinetics of the thermal decomposition of cellulose under the experimental conditions of thermal analysis. Theoretical extrapolations to high heating rates," *Biomass and Bioenergy* 7(1–6), 69-74. DOI: 10.1016/0961-9534(95)92631-H

Wang, S., Yu, S., Li, J., and Li, S. (2020). "Effects of functionalized nano-TiO_2 on the molecular motion in epoxy resin-based nanocomposites," *Materials* 13, aritcle 163. DOI:10.3390/ma13010163

Wang, Y., Yeh, F. C., Lai, S. M., Chan, H. C., and Shen, H. F. (2003). "Effectiveness of functionalized polyolefins as compatibilizers for polyethylene/wood flour composites," *Polymer Engineering and Science* 43(4), 933-945.

Woodhams, R. T., Law, S., and Balatinecz, J. J. (1993). "Intensive mixing of wood fibers with thermoplastics for injection-molded composites," in: *Proc. Wood Fiber/Polymer*

Composites: Fundamental Concepts, Processes, and Material Options, M. P. Wolcott (ed.), Forest Product Society, Madison, WI, USA.

Wu, H., Xu, D., Zhou, Y., Gao, C., Guo, J., He, W., He, Y., and Qin, S. (2020). "Tung oil anhydride modified hemp fiber/polypropylene composites: The improved toughness, thermal stability and rheological property," *Fibers and Polymers* 21(9), 2084-2091. DOI: 10.1007/s12221-020-1157-1

Xiang, X., Xiang, D., Fang, W., and Ma, J. (2012). "Friction and wear behavior of POM composites filled with LDPE and wood fibers," *Advanced Materials Research*, Vols. 415-417, 293-296. DOI: 10.4028/www.scientific.net/AMR.415-417.293

Yam, K. L., Gogoi, B. K., Lai, C. C., and Selke, S. E. (1990). "Composites from compounding wood fibers with recycled high density polyethylene," *Polymer Engineering & Science* 30(11), 693-699. DOI: 10.1002/pen.760301109

Yang, H. S., Wolcott, M. P., Kim, H. S., Kim, S., and Kim, H. J. (2007). "Effect of different compatibilizing agents on the mechanical properties of lignocellulosic material filled polyethylene bio-composites," *Composite Structures* 79, 369-375. DOI: 10.1016/j.compstruct.2006.02.016

Yang, Z., Guo, Z., and Yuan, C. (2019). "Tribological behavior of polymer composites functionalized with various microcapsule core materials," *Wear* Vol. 426-427, 853-861. DOI: 10.1016/j.wear.2019.01.107

Yetgin, S. H. (2020). "Tribological properties of compatabilizer and graphene oxide-filled polypropylene nanocomposites," *Bulletin of Materials Science* 43(1), article 89. DOI: 10.1007/s12034-020-2061-4

Yousif, B. F., and El-Tayeb, N. S. M. (2008). "High-stress three-body abrasive wear of treated and untreated oil palm fibre-reinforced polyester composites," *Proceedings of the Institution of Unauthenticated Mechanical Engineers, Part C: Journal of Mechanical Engineering Science* 222(5), 637-646. DOI: 10.1243/13506501JET412

Yousif, B. F., and El-Tayeb, N. S. M. (2010). "Wet adhesive wear characteristics of untreated oil palm fibre-reinforced polyester and treated oil palm fibre-reinforced polyester composites using the pin-on-disc and block-on-ring techniques," *Proceedings of the Institution of Mechanical Engineers, Part J: Journal of Engineering Tribology* 224(2), 123-131. DOI: 10.1243/13506501JET655

Yousif, E., and Haddad, R. (2013). "Photodegradation and photostabilization of polymers, especially polystyrene: Review," *SpringerPlus* 2(1), article 398. DOI: 10.1186/2193-1801-2-398

Yuan, Q., Wu, D., Gotama, J., and Bateman, S. (2008). "Wood fiber reinforced polyethylene and polypropylene composites with high modulus and impact strength," *Journal of Thermoplastic Composite Materials* 21(3), 195-208. DOI: 10.1177/0892705708089472

Article submitted: June 18, 2023; Peer review completed: August 12, 2023; Revised version received and accepted: August 22, 2023; Published: August 30, 2023.
DOI: 10.15376/biores.18.4.7251-7294